

EFFECTIVE NUCLEAR OPERATORS WITH THE
COUPLED-CLUSTER METHOD

By

Samuel John Novario

A DISSERTATION

Submitted to
Michigan State University
in partial fulfillment of the requirements
for the degree of

Physics—Doctor of Philosophy

2017

PUBLIC ABSTRACT

EFFECTIVE NUCLEAR OPERATORS WITH THE COUPLED-CLUSTER METHOD

By

Samuel John Novario

Your public abstract goes here. This is a preview of the dissertation/thesis template. General instructions for the template can be found in Chapter 7.

—

Lorem ipsum dolor sit amet, consectetur adipiscing elit. Vivamus tristique pretium ipsum nec bibendum. Vestibulum eleifend viverra dui, non molestie libero tincidunt a. Duis commodo odio eget rhoncus cursus. Quisque mattis scelerisque purus in facilisis. Ut consectetur luctus venenatis. Phasellus pulvinar congue tellus, eu tempor augue congue at. In hac habitasse platea dictumst. In accumsan tristique neque quis convallis. Duis quis portitor orci. Vestibulum ante ipsum primis in faucibus orci luctus et ultrices posuere cubilia Curae; Sed sit amet elit sit amet elit scelerisque mattis. Nam a cursus sapien.

ABSTRACT

EFFECTIVE NUCLEAR OPERATORS WITH THE COUPLED-CLUSTER METHOD

By

Samuel John Novario

Your abstract goes here. This is a preview of the dissertation/thesis template. General instructions for the template can be found in Chapter 7.

—

Lorem ipsum dolor sit amet, consectetur adipiscing elit. Vivamus tristique pretium ipsum nec bibendum. Vestibulum eleifend viverra dui, non molestie libero tincidunt a. Duis commodo odio eget rhoncus cursus. Quisque mattis scelerisque purus in facilisis. Ut consectetur luctus venenatis. Phasellus pulvinar congue tellus, eu tempor augue congue at. In hac habitasse platea dictumst. In accumsan tristique neque quis convallis. Duis quis portitor orci. Vestibulum ante ipsum primis in faucibus orci luctus et ultrices posuere cubilia Curae; Sed sit amet elit sit amet elit scelerisque mattis. Nam a cursus sapien.

(Only needed if you intend
to register for a copyright.)

Copyright by
SAMUEL JOHN NOVARIO
2017

Your dedication goes here. It is optional.

Lorem ipsum dolor sit amet, consectetur adipiscing elit. Donec mollis mauris vitae massa
aliquet, at accumsan lorem lobortis.

ACKNOWLEDGMENTS

Your acknowledgments goes here. It is optional. You can also use the variant spelling “Acknowledgements” (note the extra “e”).

—

Lorem ipsum dolor sit amet, consectetur adipiscing elit. Donec vel nisl aliquam, tincidunt lacus et, sollicitudin lectus. Mauris quis sagittis risus. Lorem ipsum dolor sit amet, consectetur adipiscing elit. Vestibulum aliquet odio leo, eget laoreet leo dictum luctus. Aliquam at nisi eu turpis posuere rhoncus id ac neque. Nunc iaculis turpis id rhoncus rutrum.

In pharetra neque luctus, vestibulum diam quis, vehicula turpis. Proin magna magna, feugiat sed luctus consectetur, vehicula id erat. Phasellus non nisi ac ipsum vehicula aliquet. Proin pulvinar sit amet metus id finibus. Mauris et justo et mi sollicitudin commodo. Cras tempus interdum lectus ac iaculis. Proin purus purus, euismod non magna aliquet, gravida volutpat velit. Praesent eu erat purus. Cras tempus eu dolor vitae malesuada.

PREFACE

Your preface goes here. It is optional. This is a preview of the dissertation/thesis template. General instructions for the template can be found in Chapter 7.

Lorem ipsum dolor sit amet, consectetur adipiscing elit. In id pellentesque lacus. Praesent scelerisque eros sit amet felis faucibus pretium. Pellentesque cursus maximus consectetur. Suspendisse at congue eros. Cras tincidunt tellus lorem, ut viverra ligula sagittis eget. Praesent egestas viverra leo a rutrum. Vivamus finibus magna eu sapien tristique, eget congue mi facilisis. Integer porttitor dignissim dolor ut porta. Nulla congue hendrerit nulla, et volutpat elit scelerisque vitae.

Donec convallis, nunc eget efficitur lacinia, magna ipsum dignissim dolor, vitae mollis neque sem in ipsum. In quam mi, laoreet ac nibh sed, imperdiet tincidunt tellus. Sed dictum ante ac facilisis ornare. Curabitur sit amet purus quis nulla dictum blandit in ut purus. Praesent eget ligula in nisl interdum facilisis vitae vitae magna. Ut quis ornare augue. Cras aliquet ac ex iaculis rutrum. Vestibulum volutpat fermentum orci, sed laoreet neque auctor eu. Fusce ac lorem congue, blandit eros a, tincidunt leo. Cras luctus ultricies mollis. Phasellus laoreet nulla sit amet ipsum sollicitudin facilisis. Donec sit amet est volutpat, accumsan nisi sed, fringilla mi.

TABLE OF CONTENTS

LIST OF TABLES	ix
LIST OF FIGURES	x
KEY TO SYMBOLS AND ABBREVIATIONS	xi
Chapter 1 Introduction	1
1.1 A Brief History of Nuclear Structure Theory	2
1.2 Electroweak Theory and Nuclear Structure	3
1.3 Ab-Initio Descriptions of Beta Decay	6
1.4 Thesis Structure	6
Chapter 2 Many-Body Quantum Mechanics	8
2.1 Many-Body Perturbation Theory	9
2.2 Many-Body Perturbation Theory	11
Chapter 3 Coupled-Cluster Theory	17
Chapter 4 Equation-of-Motion Method	35
Chapter 5 Effective Operators	44
5.1 Beta Decay	46
Chapter 6 Conclusions and Perspectives	47
Chapter 7 Instructions	48
7.1 Preamble	48
7.2 Front matter	49
7.3 Main matter	49
Chapter 8 Appendix	50
Chapter 9 Lorem ipsum	51
9.1 Pellentesque Scelerisque	51
9.1.1 Fusce Convallis	52
9.2 Curabitur	53
APPENDICES	55
Appendix A Etiam a Convallis	56
Appendix B Nulla Feugiat	58
Appendix C Angular Momentum Coupling	59
Appendix D Coupled Two-Body State	60
Appendix E Convergence Acceleration: Direct-Inversion of the Iterative Subspace	61

Appendix F CCSD Diagrams	62
Appendix G Computational Implementation	69
REFERENCES	77

LIST OF TABLES

Table 9.1:	Nulla suscipit ultricies massa at sagittis.	54
Table B.1:	Lorem ipsum dolor sit amet, consectetur adipiscing elit. Nulla feugiat ante quis consectetur pellentesque. In tincidunt orci in justo tempor, non tempor metus congue.[25]	58

LIST OF FIGURES

Figure 1.1:	Nuclear Chart blah blah blah ab-initio	4
Figure 1.2:	ab-initio progress blah blah blah	5
Figure 3.1:	(Color online) Diagrammatic representation of \bar{H} of Eq. (3.10), excluding terms involving the one-body interaction \hat{H}_1 and first-order terms involving only the bare Hamiltonian. Open circles represent the excitation cluster operators \hat{T}_1 and \hat{T}_2 , and filled circles represent the two-body interaction \hat{H}_2 . As before, the diagrams are implicitly antisymmetrized (Hugenholtz diagrams). Lines connected to \hat{T} are always directed upward because they represent an excitation operator while the directions of external lines connected to \hat{H}_2 are unconstrained.	22
Figure 9.1:	Lorem ipsum dolor sit amet, consectetur adipiscing elit. Ut et leo non tortor viverra sodales.	52
Figure 9.2:	Ut condimentum odio orci, a varius sapien vehicula quis.	52

KEY TO SYMBOLS AND ABBREVIATIONS

$Ap-Bh$ A -particle, B -hole excitation or de-excitation from the reference state

$|0\rangle$ vacuum state

$|\Phi\rangle$ reference state

$|\Psi\rangle$ correlated ground state

$|\Phi_{i_1 \dots i_B}^{a_1 \dots a_A}\rangle$ specific $Ap-Bh$ state

$\{\dots\}$ normal-ordered with respect to the reference state

$\hbar\omega$ harmonic oscillator energy scale

\hat{H} Hamiltonian

\bar{H} similarity-transformed Hamiltonian

\hat{H}_N normal-ordered Hamiltonian

\bar{H}_N normal-ordered similarity-transformed Hamiltonian

\hat{T} cluster operator

$\varepsilon_{i_1 \dots i_B}^{a_1 \dots a_A}$ energy denominator, $f_{i_1}^{i_1} + \dots + f_{i_B}^{i_B} - f_{a_1}^{a_1} - \dots - f_{a_A}^{a_A}$

CC coupled cluster

CCD coupled cluster with doubles

CCSD coupled cluster with singles and doubles

CCSDT coupled cluster with singles, doubles, and triples

CCSD(T) coupled cluster with singles, doubles, and triples approximation

Λ -CCSD(T) coupled cluster with singles, doubles, and Λ -triples approximation

CI configuration interaction

FCI full configuration interaction

COM center of mass

EOM equations-of-motion

PA particle-attached

PR particle-removed
EOM equations-of-motion
EOM-CC equations-of-motion coupled cluster
EOM-CCSD equations-of-motion coupled cluster with singles and doubles
HF Hartree-Fock
IM-SRG in-medium similarity renormalization group
HO harmonic oscillator
LECs low-energy constants
MBPT many-body perturbation theory
WS Woods-Saxon
DIIS direct-inversion of the iterative subspace
QCD quantum chromodynamics
EFT effective field theory
NN nucleon-nucleon
3N three-nucleon
NLO next-to leading order
N²LO next-to-next-to leading order
N³LO next-to-next-to-next-to leading order

Chapter 1

Introduction

Steady progress in any modern scientific endeavor requires a strong, dynamic relationship between experimental data to paint an accurate picture of some natural phenomena and theoretical models to interpret those phenomena with respect to the growing network of other scientific models. Conversely, the predictive capability of theoretical models can highlight blurry or unfinished areas of that picture which can be clarified or completed by new or improved experimental techniques. In the pursuit to understand and describe the atomic nucleus and the corresponding implications from quarks to neutron stars, this push-and-pull coordination between theory and experiment makes progress in modern nuclear physics robust and persistent.

An integral component of modern nuclear physics is describing the structure and emergent properties of self-bound systems of protons and neutrons. The systems in questions can be stable nuclei, rare isotopes far from stability, and even infinite nuclear matter which can be used to model neutron stars. Relevant properties to nuclear structure include ground-state energies—for determining nuclear masses, excited-state energies—for identification in gamma or neutron spectroscopy, and transition or decay amplitudes—for calculating the respective rates for those processes. This wide array of emergent properties inserts both nuclear structure theory and experiment into a prominent role within every other subfield of modern nuclear physics, from lattice quantum chromodynamics (QCD) to nuclear astrophysics, and beyond, to questions about fundamental symmetries and dark matter. However, two inextricable characteristics of a comprehensive model of nuclear structure—the increasingly large

size of many-body nuclear systems and the complexity and strength of the nucleon-nucleon interactions—have been imposing hurdles for theorists to overcome.

1.1 A Brief History of Nuclear Structure Theory

The project to solve the correlation problem in many-fermion systems began with the work of Brueckner, Bethe, and Goldstone [14, 8, 1] with the reformulation of the nuclear interaction by accounting for two-body correlations from the nuclear medium. This work continued with the work of Coester and Kummel [22, 23, 47] with a further resummation of nuclear correlations in the form of an exponential ansatz into what would become coupled-cluster (CC) theory. However, there were two major obstacles that hindered the progress in this area for decades. First, while these methods were systematically improvable by including progressively higher-level correlations, the highly-nonperturbative nature of the nuclear force required computationally infeasible summations. Second, there wasn't a reliable and consistent theory to model nucleon-nucleon interactions.

However, the well-known and highly-perturbative Coulomb force, which underlies the many-electron systems in atoms and molecules, made consistent advances in ab-initio quantum chemistry possible since the 1950s. Along with the quasi-exact method of configuration interaction (CI) [64, 24, 3, 77] which physicists had utilised since the formulation of quantum mechanics, chemists successfully employed approximate methods like many-body perturbation theory (MBPT) [39, 40, 62, 63] and coupled-cluster theory [20, 18, 19, 55, 63].

Fortunately, within the past decade, two breakthroughs allowed ab-initio nuclear structure to resurface and thrive the way that quantum chemistry had done. The first was the invention of chiral effective field theory (EFT) [27, 50] which gave theorists the ability to construct nucleon-nucleon interactions consistent with the underlying QCD of the strong

nuclear force. The second was the application of renormalization group (RG) methods to the nuclear force [12, 61]. This procedure “softens” the NN interaction, which decouples the high- and low-momentum components of the nuclear force and generates less-correlated systems that can be calculated at a reasonable computational cost. These major changes to nuclear structure theory made it possible to merge the field with the progress of quantum chemistry and open a new area for additional developments in ab-initio descriptions of many-fermion systems.

no-core shell model NCSM [52, 53, 5] quantum Monte Carlo QMC [57, 56, 17]

modern CC [78, 79, 41, 42, 31, 46, 29, 9] modern IMSRG [75, 76, 36, 11, 37, 35, 69, 68]

self-consistent Green’s function SCGF [65, 66, 67]

1.2 Electroweak Theory and Nuclear Structure

Nuclear structure is implicated in performing and analyzing experiments to probe fundamental symmetries and physics beyond the Standard Model. One example is determining the V_{ud} component of the Cabbibo-Kobayashi-Maskawa (CKM) matrix, which relates quark eigenstates of the weak interaction to their mass eigenstates [16, 44]. This matrix element can be determined from by measuring the half-lives of superallowed Fermi beta decays [71] and applying a nucleus-dependent structure correction [72, 74, 73, 4, 43]. The value of $|V_{ud}|$ is used to test the unitarity of the CKM matrix and the conserved-vector current hypothesis, which relates the ft -values of superallowed Fermi beta decays of different nuclei, both predicted by the standard model [33].

Another example of physics beyond the standard model is the neutrinoless double-beta decay ($0\nu\beta\beta$) [70, 2]. The extremely rare two-neutrino double-beta decay ($2\nu\beta\beta$) has been observed in many experiments [26, 51], have motivated the search for its neutrinoless coun-

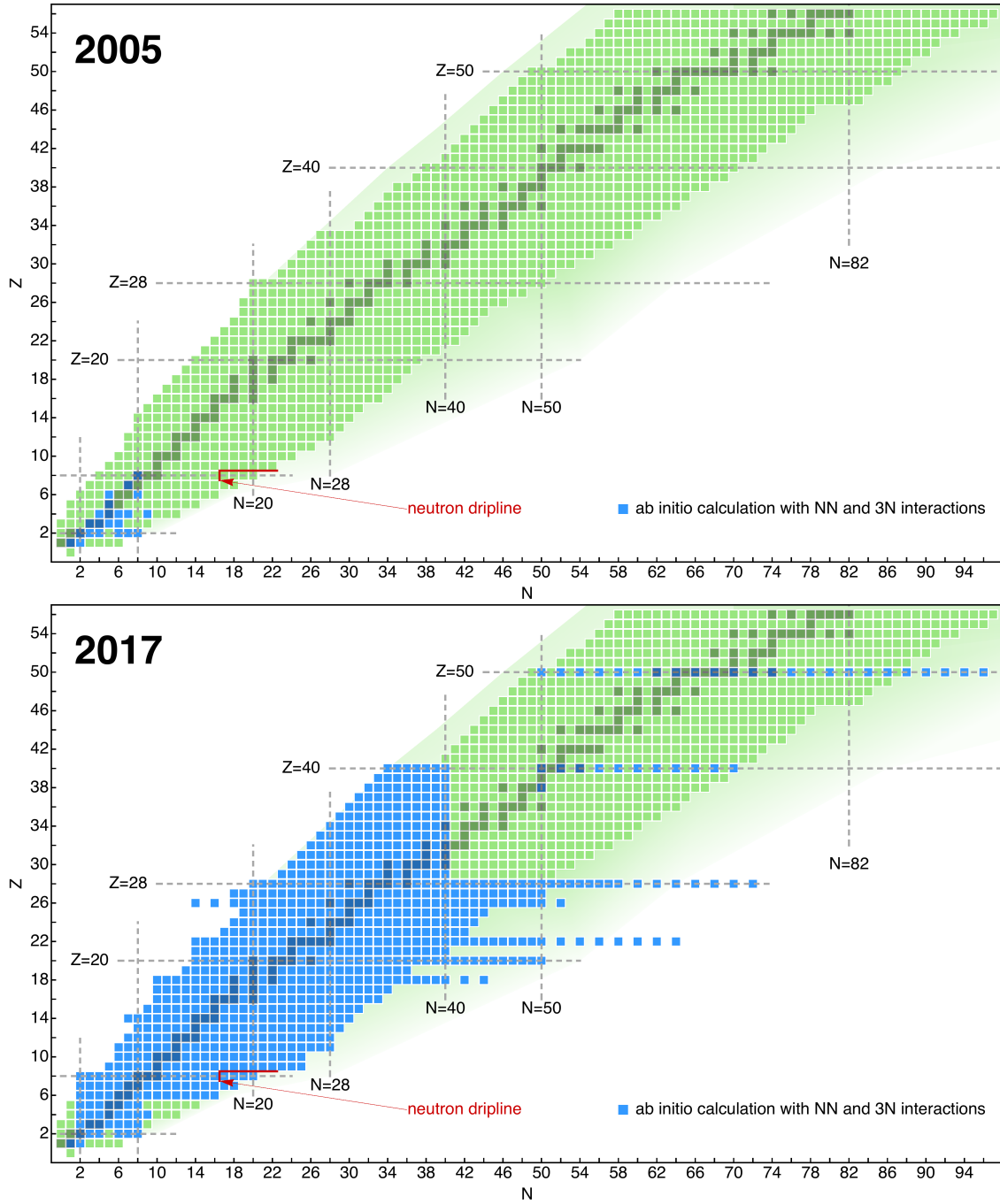


Figure 1.1: Nuclear Chart blah blah blah ab-initio

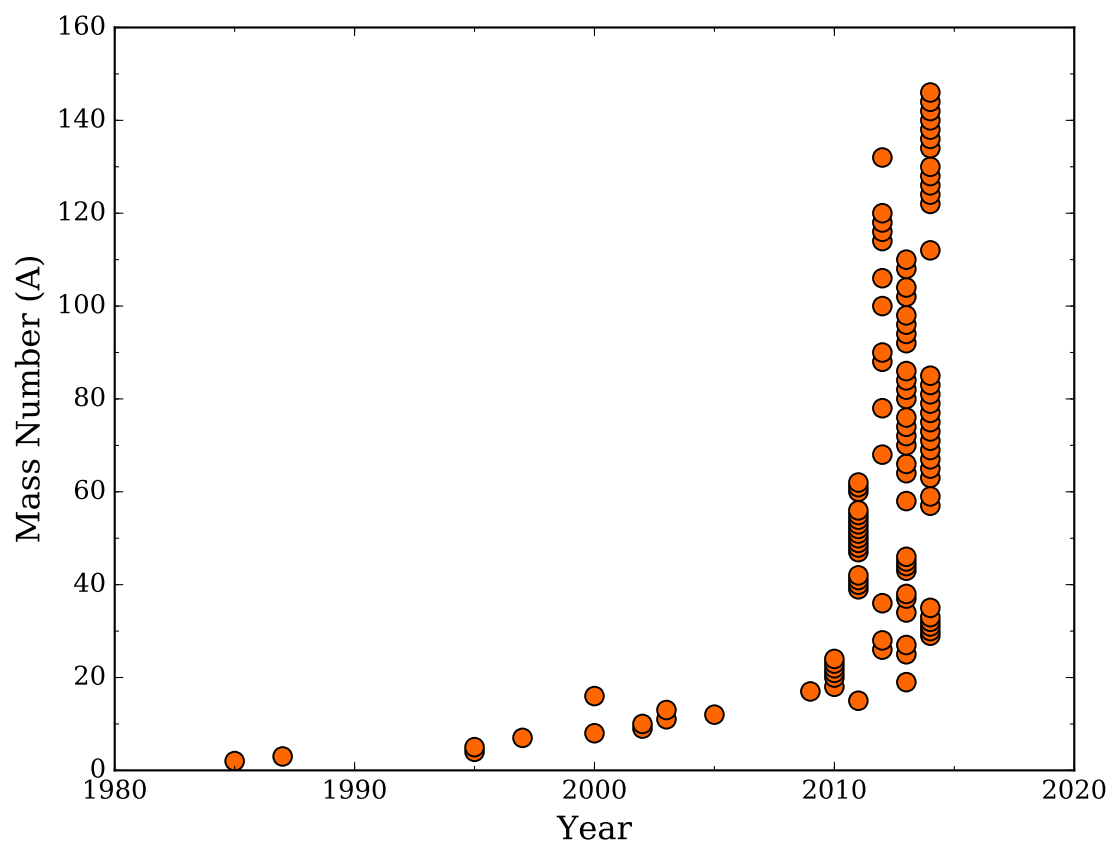


Figure 1.2: ab-initio progress blah blah blah

terpart, in which a two majorana neutrinos—being their own antiparticles—annihilate one another, which is not possible in the standard electro-weak theory. The long half-lives of these theoretical decays depend on a phase-space factor, which is highly dependent on the decay Q -value, and a nuclear matrix element. The Q -value can be determined from high-precision mass measurements of the relevant nuclei [49, 30, 60, 15], while the nuclear matrix element, which contributes the largest source of uncertainty, must be calculated with a sufficient many-body theory.

The weak interaction and nuclear structure can also be exploited for supernova neutrino detection and spectroscopy. While these original detectors were based on electron-neutrino scattering [38, 10], more recent experiments utilize correlated nucleon effects of large nuclei to enhance the scattering cross section and therefore the ability to resolve energies and distinguish neutrino flavors [34, 21, 28, 48]. Supernova models predict distinct distributions for different neutrino flavors based on the temperatures at which they are emitted [45, 7]. With nuclear structure calculations that include sufficient nuclear correlations, these high-resolution detectors can be used to verify specific models.

1.3 Ab-Initio Descriptions of Beta Decay

1.4 Thesis Structure

The main goal of this work is to explore the ab initio description of beta decay within the coupled-cluster theory framework of EOM-CCSD using renormalized chiral NN and 3N interactions. The organization of the thesis builds from a general description of the many-body problem of quantum mechanics in chapter 2 2. Then, in chapter 3 3, this many-body framework is applied within the coupled-cluster theory an applied to various systems

including the atomic nucleus. In chapter 4 4, the coupled-cluster method is extended to the equations-of-motion methods to describe open-shell systems. Chapter 5 5 outlines the procedure to express observables as effective coupled-cluster operators and how to calculate those observables in the equations-of-motion framework. Then, in chapter 6 5.1, the ability to calculate effective operators is applied to Fermi- and Gamow-Teller- beta-decay operators and relevant quantities are determined for various nuclei. Lastly, conclusions and future perspectives are given in chapter 7 6 while technical details concerning the formalism and implementation are given in the appendix 8.

Chapter 2

Many-Body Quantum Mechanics

$$\Phi_0(\vec{r}_1, \dots, \vec{r}_A) = \frac{1}{\sqrt{A!}} \begin{vmatrix} \phi_1(\vec{r}_1) & \phi_1(\vec{r}_2) & \cdots & \phi_1(\vec{r}_A) \\ \phi_2(\vec{r}_1) & \phi_2(\vec{r}_2) & \cdots & \phi_2(\vec{r}_A) \\ \vdots & \vdots & \ddots & \vdots \\ \phi_A(\vec{r}_1) & \phi_A(\vec{r}_2) & \cdots & \phi_A(\vec{r}_A) \end{vmatrix} \quad (2.1)$$

$$V_{\text{WS}}(r) = -V_0 \left[1 + e^{\frac{(r-R_0)}{a}} \right]^{-1} \quad (2.2)$$

$$V_{\text{HO}}(r) = \frac{1}{2} m \omega^2 r^2 \quad (2.3)$$

$$\hat{H} = {}^{(1)}\hat{H} + {}^{(2)}\hat{H} + {}^{(3)}\hat{H} + \dots \quad (2.4)$$

$$\hat{H} = \frac{-\hbar^2}{2m} \sum_i^A \nabla_i^2 + \sum_{i < j}^A {}^{(2)}\hat{H}(\vec{r}_i, \vec{r}_j) + \sum_{i < j < k}^A {}^{(3)}\hat{H}(\vec{r}_i, \vec{r}_j, \vec{r}_k) + \dots \quad (2.5)$$

$$\hat{H} = \sum_{pq} {}^{(1)}H_q^p \hat{p}^\dagger \hat{q} + \frac{1}{4} \sum_{pqrs} {}^{(2)}H_{rs}^{pq} \hat{p}^\dagger \hat{q}^\dagger \hat{s} \hat{r} + \frac{1}{36} \sum_{pqrst} {}^{(3)}H_{stu}^{pqr} \hat{p}^\dagger \hat{q}^\dagger \hat{r}^\dagger \hat{u} \hat{t} \hat{s} + \dots \quad (2.6)$$

$$\hat{H} = E_0 + \sum_{pq} f_q^p \left\{ \hat{p}^\dagger \hat{q} \right\} + \frac{1}{4} \sum_{pqrs} V_{rs}^{pq} \left\{ \hat{p}^\dagger \hat{q}^\dagger \hat{s} \hat{r} \right\} + \frac{1}{36} \sum_{pqrstu} W_{stu}^{pqr} \left\{ \hat{p}^\dagger \hat{q}^\dagger \hat{r}^\dagger \hat{u} \hat{t} \hat{s} \right\} + \dots \quad (2.7)$$

$$E_0 = \sum_i {}^{(1)}H_i^i + \frac{1}{2} \sum_{ij} {}^{(2)}H_{ij}^{ij} + \frac{1}{6} \sum_{ijk} {}^{(3)}H_{ijk}^{ijk} \dots \quad (2.8)$$

$$f_q^p = {}^{(1)}H_q^p + \sum_i {}^{(2)}H_{qi}^{pi} + \frac{1}{2} \sum_{ij} {}^{(3)}H_{qij}^{pij} + \dots \quad (2.9)$$

$$V_{rs}^{pq} = {}^{(2)}H_{rs}^{pq} + \sum_i {}^{(3)}H_{rsi}^{pqi} + \dots \quad (2.10)$$

$$W_{stu}^{pqr} = {}^{(3)}H_{stu}^{pqr} + \dots \quad (2.11)$$

2.1 Many-Body Perturbation Theory

$$\hat{H} = \hat{H}_0 + \hat{H}_1 \quad (2.12)$$

$$\hat{H}|\Psi\rangle = (\hat{H}_0 + \hat{H}_1) |\Psi\rangle = E|\Psi\rangle \quad (2.13)$$

$$\langle \Phi | \hat{H} | \Psi \rangle = \langle \Psi | (\hat{H}_0 + \hat{H}_1) | \Psi \rangle = E \quad (2.14)$$

$$\langle \Phi | \hat{H}_0 | \Psi \rangle + \langle \Phi | \hat{H}_1 | \Psi \rangle = E \langle \Phi | \Psi \rangle = E \quad (2.15)$$

$$\hat{H}_0 | \Phi \rangle = E^{(0)} | \Phi \rangle \quad (2.16)$$

$$\langle \hat{H}_0 \Phi | \Psi \rangle + \langle \Phi | \hat{H}_1 | \Psi \rangle = E^{(0)} \langle \Phi | \Psi \rangle + \langle \Phi | \hat{H}_1 | \Psi \rangle = E^{(0)} + \langle \Phi | \hat{H}_1 | \Psi \rangle = E \quad (2.17)$$

$$\Delta E \equiv E - E^{(0)} = \langle \Phi | \hat{H}_1 | \Psi \rangle \quad (2.18)$$

$$(\hat{H} - E) \Psi = 0 \quad (2.19)$$

$$E \equiv E^{(0)} + \Delta E = E^{(0)} + \lambda E^{(1)} + \lambda^2 E^{(2)} + \dots \quad (2.20)$$

$$\Psi \equiv \Phi + \mathcal{X} = \mathcal{X}^{(0)} + \lambda \mathcal{X}^{(1)} + \lambda^2 \mathcal{X}^{(2)} + \dots \quad (2.21)$$

$$(\hat{H}_0 + \lambda \hat{H}_1 - E^{(0)} - \lambda E^{(1)} - \lambda^2 E^{(2)} - \dots) (\mathcal{X}^{(0)} + \lambda \mathcal{X}^{(1)} + \lambda^2 \mathcal{X}^{(2)} + \dots) = 0 \quad (2.22)$$

$$(\hat{H}_0 - E^{(0)}) \mathcal{X}^{(0)} = 0 \quad (2.23)$$

$$(\hat{H}_0 - E^{(0)}) \mathcal{X}^{(1)} + (\hat{H}_1 - E^{(1)}) \mathcal{X}^{(0)} = 0 \quad (2.24)$$

$$(\hat{H}_0 - E^{(0)}) \mathcal{X}^{(2)} + (\hat{H}_1 - E^{(1)}) \mathcal{X}^{(1)} - E^{(2)} \mathcal{X}^{(0)} = 0 \quad (2.25)$$

$$(\hat{H}_0 - E^{(0)}) \mathcal{X}^{(n)} + (\hat{H}_1 - E^{(1)}) \mathcal{X}^{(n-1)} - \sum_{m=0}^{n-2} E^{(n-m)} \mathcal{X}^{(m)} = 0 \quad (2.26)$$

$$\langle \Phi | (\hat{H}_0 - E^{(0)}) | \mathcal{X}^{(n)} \rangle = \langle \Phi | (E^{(1)} - \hat{H}_1) | \mathcal{X}^{(n-1)} \rangle + \langle \Phi | \sum_{m=0}^{n-2} E^{(n-m)} | \mathcal{X}^{(m)} \rangle \quad (2.27)$$

$$\langle \Phi | \hat{H}_0 | \mathcal{X}^{(n)} \rangle - \langle \Phi | E^{(0)} | \mathcal{X}^{(n)} \rangle = \langle \Phi | E^{(1)} | \mathcal{X}^{(n-1)} \rangle - \langle \Phi | \hat{H}_1 | \mathcal{X}^{(n-1)} \rangle + \sum_{m=0}^{n-2} \langle \Phi | E^{(n-m)} | \mathcal{X}^{(m)} \rangle \quad (2.28)$$

$$\langle \Phi | \hat{H}_0 | \mathcal{X}^{(n)} \rangle - \langle \Phi | E^{(0)} | \mathcal{X}^{(n)} \rangle = -\langle \Phi | \hat{H}_1 | \mathcal{X}^{(n-1)} \rangle + \sum_{m=0}^{n-1} \langle \Phi | E^{(n-m)} | \mathcal{X}^{(m)} \rangle \quad (2.29)$$

$$(E^{(0)} - E^{(0)}) \langle \Phi | \mathcal{X}^{(n)} \rangle = -\langle \Phi | \hat{H}_1 | \mathcal{X}^{(n-1)} \rangle + \sum_{m=0}^{n-1} E^{(n-m)} \langle \Phi | \mathcal{X}^{(m)} \rangle \quad (2.30)$$

$$0 = -\langle \Phi | \hat{H}_1 | \mathcal{X}^{(n-1)} \rangle + \sum_{m=0}^{n-1} E^{(n-m)} \delta_{m0} \quad (2.31)$$

$$E^{(n)} = \langle \Phi | \hat{H}_1 | \mathcal{X}^{(n-1)} \rangle \quad (2.32)$$

$$E^{(1)} = \langle \Phi | \hat{H}_1 | \Phi \rangle \quad (2.33)$$

$$E^{(n)} = \langle \Phi | \hat{H}_1 | \mathcal{X}^{(n-1)} \rangle \quad (2.34)$$

2.2 Many-Body Perturbation Theory

Many-body perturbation theory treats the interaction part of the Hamiltonian, H_1 , as a perturbation using the parameter λ to keep track of the perturbation order. The unperturbed Hamiltonian is given when $\lambda = 0$ and the full Hamiltonian is restored when $\lambda = 1$,

$$H = H_0 + \lambda H_1. \quad (2.35)$$

The solution wave functions to the unperturbed Hamiltonian are given by Φ_n and those for the perturbed Hamiltonian are given by Ψ_n ,

$$H_0 |\Phi_n\rangle = E_n^{(0)} |\Phi_n\rangle \quad (2.36)$$

$$(H_0 + H_1) |\Psi_n\rangle = E_n |\Psi_n\rangle \quad (2.37)$$

If one assumes that the Φ_n are non-degenerate, then the perturbed wave functions and energies become the corresponding non-perturbed wave function and energies when $\lambda \rightarrow 0$. Defining the differences between the full and unperturbed wave functions and energies as $\chi_n = \Psi_n - \Phi_n$ and $\Delta E_n = E_n - E_n^{(0)}$, respectively, I can rewrite the Schrodinger equation as

$$H (\Phi_n + \chi_n) = E_n (\Phi_n + \chi_n) \quad (2.38)$$

$$(H - E_n) \chi_n = (E_n - H) \Phi_n = (E_n - H_0 - H_1) \Phi_n \quad (2.39)$$

$$(H - E_n) \chi_n = (E_n - E_n^{(0)} - H_1) \Phi_n = (\Delta E_n - H_1) \Phi_n \quad (2.40)$$

Because any solution to the homogeneous version of Eqn. (28), $(H - E_n) \chi_n = 0$, can be added to the solution of the inhomogeneous version, there exists a degree of freedom that can be used to set χ_n orthogonal to Φ_n , $\langle \chi_n | \Phi_n \rangle = 0$. This form is known as intermediate normalization and sets the following inner products,

$$\langle \Phi_n | \Psi_n \rangle = \langle \Phi_n | \Phi_n + \chi_n \rangle = \langle \Phi_n | \Phi_n \rangle + \langle \Phi_n | \chi_n \rangle = 1 + 0 = 1, \quad (2.41)$$

$$\langle \Psi_n | \Psi_n \rangle = \langle \Phi_n + \chi_n | \Phi_n + \chi_n \rangle = \langle \Phi_n | \Phi_n \rangle + \langle \chi_n | \chi_n \rangle = 1 + \langle \chi_n | \chi_n \rangle. \quad (2.42)$$

Now the perturbation expansion equations can be written by first expanding χ_n and ΔE_n in different orders of λ where the zero-order contributions correspond to the unperturbed wave function and energy, respectively.

$$\Psi_n = \Phi_n + \chi_n = \Psi_n^{(0)} + \lambda \Psi_n^{(1)} + \lambda^2 \Psi_n^{(2)} + \dots \quad (2.43)$$

$$E_n = E_n^{(0)} + \Delta E_n = E_n^{(0)} + \lambda E_n^{(1)} + \lambda^2 E_n^{(2)} + \dots \quad (2.44)$$

Plugging these expansions into the perturbed Hamiltonian, $(H_0 + \lambda H_1 - E_n) \Psi_n = 0$, gives

$$(H_0 + \lambda H_1 - E_n^{(0)} - \lambda E_n^{(1)} - \lambda^2 E_n^{(2)} - \dots) (\Psi_n^{(0)} + \lambda \Psi_n^{(1)} + \lambda^2 \Psi_n^{(2)} + \dots) = 0 \quad (2.45)$$

After expanding the expressions in Eqn. (33), different orders of λ can be equated to give order-by-order equations for the $\Psi_n^{(m)}$ in terms of the lower-order wave functions. In general, the equations are given by

$$(E_n^{(0)} - H_0) \Psi_n^{(0)} = 0, \quad (2.46)$$

$$(E_n^{(0)} - H_0) \Psi_n^{(m)} = H_1 \Psi_n^{(m-1)} - \sum_{l=0}^{m-1} E_n^{(m-l)} \Psi_n^{(l)}. \quad (2.47)$$

The corresponding order-by-order energies are solved by multiplying Eqn. (35) by $\langle \Phi_n |$ and integrating,

$$\langle \Phi_n | (E_n^{(0)} - H_0) | \Psi_n^{(m)} \rangle = \langle \Phi_n | H_1 | \Psi_n^{(m-1)} \rangle - \sum_{l=0}^{m-1} E_n^{(m-l)} \langle \Phi_n | \Psi_n^{(l)} \rangle. \quad (2.48)$$

The first term is zero because it gives the solution to the unperturbed Hamiltonian, and the inner product in the last term is only non-zero when $l = 0$,

$$E_n^{(m)} = \langle \Phi_n | H_1 | \Psi_n^{(m-1)} \rangle. \quad (2.49)$$

We see here that the n^{th} order wavefunction contains the perturbation to the $n - 1^{\text{th}}$ order.

Using another formulation more conducive to many-body techniques, we start by introducing the projection operator Q which projects out the unperturbed reference wave function, $|\Phi_0\rangle$, from any state.

$$Q = \sum_{n \neq 0} |\Phi_n\rangle \langle \Phi_n| = 1 - |\Phi_0\rangle \langle \Phi_0| \quad (2.50)$$

It's easy to show that this projection operator commutes with $(E_n^{(0)} - H_0)$,

$$Q(E_n^{(0)} - H_0) = (1 - |\Phi_0\rangle \langle \Phi_0|)(E_n^{(0)} - H_0) = (E_n^{(0)} - H_0) - |\Phi_0\rangle \langle \Phi_0| (E_n^{(0)} - H_0) \quad (2.51)$$

$$= (E_n^{(0)} - H_0) - |\Phi_0\rangle \langle \Phi_0| (E_n^{(0)} - E_0^{(0)}) = (E_n^{(0)} - H_0) - (E_n^{(0)} - E_0^{(0)}) |\Phi_0\rangle \langle \Phi_0| \quad (2.52)$$

$$= (E_n^{(0)} - H_0) - (E_n^{(0)} - H_0) |\Phi_0\rangle \langle \Phi_0| = (E_n^{(0)} - H_0) (1 - |\Phi_0\rangle \langle \Phi_0|) = (E_n^{(0)} - H_0) Q \quad (2.53)$$

This implies that

$$(E_n^{(0)} - H_0) Q |\Psi_n\rangle = Q (E_n^{(0)} - H_0) |\Psi_n\rangle = Q (E_n^{(0)} - H + H_1) |\Psi_n\rangle = Q (E_n^{(0)} - E_n + H_1) |\Psi_n\rangle \quad (2.54)$$

Assuming that the eigenvalues, $E_n^{(0)}$, are non-degenerate, the operator $(E_0^{(0)} - H_0)$ is singular on $|\Phi_0\rangle$ but non-singular on the Q-space. Therefore, it can be inverted in the preceding

equation,

$$Q|\Psi_0\rangle = (E_0^{(0)} - H_0)^{-1} Q (E_0^{(0)} - H + H_1) |\Psi_0\rangle = R^{(0)} (E_0^{(0)} - E_0 + H_1) |\Psi_0\rangle, \quad (2.55)$$

where $R^{(0)} = (E_0^{(0)} - H_0)^{-1} Q$ is the reduced resolvent of the unperturbed operator H_0 . Expanding an arbitrary term of the resolvent as an infinite series and applying the unperturbed operator gives

$$\begin{aligned} (E_0^{(0)} - H_0)^{-1} |\Phi_n\rangle\langle\Phi_n| &= (E_0^{(0)})^{-1} \left(1 - \frac{H_0}{E_0^{(0)}}\right)^{-1} |\Phi_n\rangle\langle\Phi_n| = (E_0^{(0)})^{-1} \sum_{n=0}^{\infty} \left(\frac{H_0}{E_0^{(0)}}\right)^n |\Phi_n\rangle\langle\Phi_n| \\ &= (E_0^{(0)})^{-1} \sum_{n=0}^{\infty} \left(\frac{E_n^{(0)}}{E_0^{(0)}}\right)^n |\Phi_n\rangle\langle\Phi_n| = (E_0^{(0)})^{-1} \left(1 - \frac{E_n^{(0)}}{E_0^{(0)}}\right)^{-1} |\Phi_n\rangle\langle\Phi_n| = (E_0^{(0)} - E_n^{(0)})^{-1} |\Phi_n\rangle\langle\Phi_n|. \end{aligned} \quad (2.56)$$

$$(2.57)$$

From Eqn. (45), the definition of Q , and intermediate normalization ($\langle\Phi_0|\Psi_0\rangle = 1$),

$$Q|\Psi_0\rangle = |\Psi_0\rangle - |\Phi_0\rangle\langle\Phi_0|\Psi_0\rangle = |\Psi_0\rangle - |\Phi_0\rangle = R^{(0)} (E_0^{(0)} - E_0 + H_1) |\Psi_0\rangle. \quad (2.58)$$

Now we can define $W = (E_0^{(0)} - E_0 + H_1)$, drop the superscript from the reduced resolvent, and rearrange the previous equation to give,

$$|\Psi_0\rangle = |\Phi_0\rangle + RW|\Psi_0\rangle \quad (2.59)$$

This equation can be iterated resulting in

$$|\Psi_0\rangle = \sum_{n=0}^{\infty} (RW)^n |\Phi_0\rangle \quad (2.60)$$

The energy is obtained by applying the full Hamiltonian to this expression and multiplying by the unperturbed reference function to the left before applying the intermediate normalization,

$$\langle \Phi_0 | (H_0 + H_1) | \Psi_0 \rangle = \langle \Phi_0 | H_0 | \Psi_0 \rangle + \langle \Phi_0 | H_1 | \Psi_0 \rangle = \langle \Phi_0 | E_0^{(0)} | \Psi_0 \rangle + \langle \Phi_0 | H_1 | \Psi_0 \rangle \quad (2.61)$$

$$E_0 = E_0^{(0)} \langle \Phi_0 | \Psi_0 \rangle + \langle \Phi_0 | H_1 | \Psi_0 \rangle = E_0^{(0)} + \langle \Phi_0 | \sum_{n=0}^{\infty} H_1 (RW)^n | \Phi_0 \rangle \quad (2.62)$$

Chapter 3

Coupled-Cluster Theory

One of the simplest corrections is that of the Hartree–Fock (HF) method, also known as the self-consistent field (SCF) method. Using the variational principle, one can obtain an approximate ground state of a closed-shell system by minimizing the energy expectation value E_Φ with respect to some Slater determinant $|\Phi\rangle$ in an unknown single-particle basis. We shall denote each state $|p'\rangle$ in this unknown basis by a primed label p' . We assume each unknown state $|p'\rangle$ is built from a linear combination of known basis states $|p\rangle$ with an unknown unitary matrix of coefficients $C_{pp'}$.

The goal is to find the coefficients $C_{pp'}$ that minimize the *Hartree–Fock energy* E_Φ ,

$$E_\Phi = \sum_{i'} \langle i' | \hat{H}_1 | i' \rangle + \frac{1}{2} \sum_{i'j'} \langle i'j' | \hat{H}_2 | i'j' \rangle, \quad (3.1)$$

where

$$\langle p' | \hat{H}_1 | q' \rangle = \sum_{pq} C_{pp'}^* \langle p | \hat{H}_1 | q \rangle C_{qq'}, \quad (3.2)$$

$$\langle p'q' | \hat{H}_2 | r's' \rangle = \sum_{pqrs} C_{pp'}^* C_{qq'}^* \langle pq | \hat{H}_2 | rs \rangle C_{rr'} C_{ss'}, \quad (3.3)$$

Using the method of Lagrange multipliers, the minimization problem reduces to a nonlinear

equation – the self-consistent *Hartree–Fock equations*:

$$\sum_q F_{pq} C_{qp'} = C_{pp'} \varepsilon_{p'}, \quad (3.4)$$

where the *Fock matrix* F_{pq} is defined as

$$F_{pq} \equiv \langle p | \hat{H}_1 | q \rangle + \sum_{rsi'} C_{ri'}^* \langle pr | \hat{H}_2 | qs \rangle C_{si'}, \quad (3.5)$$

and $\varepsilon_{p'}$ is a vector of Lagrange multipliers. The Coulomb and exchange terms are both contained in the second term of Eq. (3.5) due to the use of antisymmetrized matrix elements.

Besides trivial cases, the HF equation is generally solved numerically using an iterative algorithm that alternates between the use of Eq. (3.5) and Eq. (3.4) to successively refine an initial guess for $C_{pp'}$ until a fixed point (self-consistency) is reached. For our calculations, we use the identity matrix as the initial guess. When convergence is too slow, methods such as DIIS [59, 58], Broyden’s method [13], or even *ad hoc* linear mixing can improve and accelerate convergence greatly. For our quantum dot cases, linear mixing was more than adequate.

HF does not provide an exact solution to problems where multi-particle correlations are present even if the single-particle basis is not truncated (infinite in size). The discrepancy between the HF energy and the exact ground state energy is often referred to as the *correlation energy*. The focus of post-HF methods such as IM-SRG or CC is to add corrections that recover parts of the correlation energy.

To make use of the HF solution as the reference state for post-HF calculations, we transform the matrix elements via Eqs. (3.2) and (3.3). In effect, this means we are no longer operating within the harmonic oscillator single-particle basis, but rather a HF-optimized

single-particle basis. However, we will omit the prime symbols as the post-HF methods are generally basis-agnostic.

$$\begin{aligned}
\tilde{\Delta}_{ai} &\equiv \Delta_{ai} - H_{aiaai}, \\
\tilde{\Delta}_{abij} &\equiv \Delta_{abij} + w_{abij}, \\
\Delta_{p_1 \dots p_k q_1 \dots q_k} &\equiv \sum_{i=1}^k (H_{p_i p_i} - H_{q_i q_i}), \\
w_{abij} &\equiv H_{abab} - H_{aiaai} - H_{bibbi} \\
&\quad + H_{ijij} - H_{ajaj} - H_{bjbj}.
\end{aligned} \tag{3.6}$$

Coupled cluster (CC) theory is based on expressing the N -particle correlated wave function $|\Psi\rangle$ using the exponential ansatz,

$$|\Psi\rangle = e^{\hat{T}} |\Phi\rangle,$$

where $|\Phi\rangle$ is the reference state as before. The cluster operator $\hat{T} \equiv \hat{T}_1 + \hat{T}_2 + \dots + \hat{T}_N$, is composed of k -particle k -hole excitation operators, \hat{T}_k ,

$$\hat{T}_k \equiv \left(\frac{1}{k!}\right)^2 \sum_{\substack{a_1 \dots a_k \\ i_1 \dots i_k}} t_{i_1 \dots i_k}^{a_1 \dots a_k} \left\{ \hat{a}_1^\dagger \dots \hat{a}_k^\dagger \hat{i}_k \dots \hat{i}_1 \right\}, \tag{3.7}$$

where the unknown matrix elements, $t_{i_1 \dots i_k}^{a_1 \dots a_k}$, are known as *cluster amplitudes* [63].

Using the CC ansatz, the Schrödinger equation,

$$\hat{H}e^{\hat{T}}|\Phi\rangle = Ee^{\hat{T}}|\Phi\rangle, \quad (3.8)$$

can be rewritten by left-multiplying by $\langle\Phi|e^{-\hat{T}}$ as,

$$\langle\Phi|\bar{H}|\Phi\rangle = E,$$

where we define a *coupled cluster effective Hamiltonian*,

$$\bar{H} \equiv e^{-\hat{T}}\hat{H}e^{\hat{T}}, \quad (3.9)$$

in which the wave operator, $e^{\hat{T}}$, acts as a similarity transform on the Hamiltonian in the same way that $\hat{U}(s)$ acts to transform the Hamiltonian in SRG methods. An important difference, however, is that the wave operator in CC, which contains no de-excitations, is not unitary, and thus \bar{H} is not Hermitian.

The effective Hamiltonian in Eq. (3.9) can be rewritten with commutators according to the Baker–Campbell–Hausdorff expansion as,

$$\bar{H} = \hat{H} + [\hat{H}, \hat{T}] + \frac{1}{2!}[[\hat{H}, \hat{T}], \hat{T}] + \frac{1}{3!}[[[\hat{H}, \hat{T}], \hat{T}], \hat{T}] + \frac{1}{4!}[[[[\hat{H}, \hat{T}], \hat{T}], \hat{T}], \hat{T}],$$

which terminates at four-nested commutators due to the two-body nature of the interaction. Like with IM-SRG, this commutator expression ensures that CC is size-extensive and contains only connected terms. In addition, because \hat{T} is an excitation operator, terms of the form $\hat{T}\hat{H}$ are disconnected and thus vanish [63]. Therefore the CC effective Hamiltonian can

be further reduced to

$$\bar{H} = \left(\hat{H} e^{\hat{T}} \right)_c, \quad (3.10)$$

where the subscript “c” indicates that only connected terms are used.

In practice, the cluster operator \hat{T} must be truncated for calculations to be computationally feasible. In this work, we use only single and double excitations,

$$\hat{T} = \hat{T}_1 + \hat{T}_2.$$

This is known as coupled cluster with singles and doubles (CCSD), with an asymptotic computational cost that scales like IM-SRG(2). This truncation has been successfully applied to many problems in quantum chemistry [6] and nuclear physics [32]. In addition, we also truncate the three-body effective Hamiltonian terms that are induced by the similarity transformation. Fig. 3.1 shows the diagrammatic representation of Eq. (3.10) in CCSD.

The unknown cluster amplitudes in CCSD, t_i^a and t_{ij}^{ab} , are calculated by left-multiplying Eq. (3.8) by $\langle \Phi_i^a | e^{-\hat{T}}$ and $\langle \Phi_{ij}^{ab} | e^{-\hat{T}}$, respectively,

$$\langle \Phi_i^a | \bar{H} | \Phi \rangle = 0, \quad (3.11)$$

$$\langle \Phi_{ij}^{ab} | \bar{H} | \Phi \rangle = 0.$$

After the Fock matrix has been diagonalized, the diagonal components of Eq. (3.11) can be separated and, after expanding the exponent in Eq. (3.10), the non-vanishing terms of the

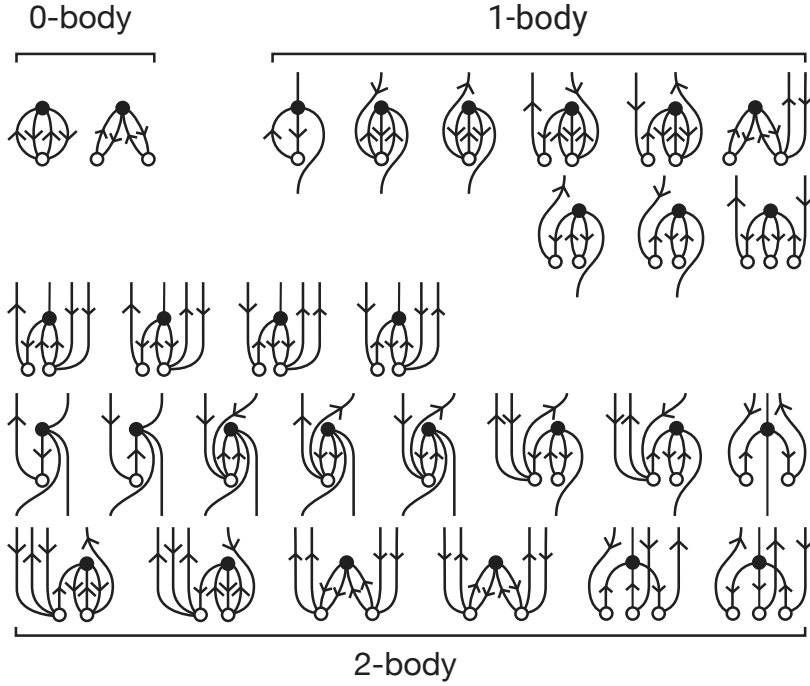


Figure 3.1: (Color online) Diagrammatic representation of \bar{H} of Eq. (3.10), excluding terms involving the one-body interaction \hat{H}_1 and first-order terms involving only the bare Hamiltonian. Open circles represent the excitation cluster operators \hat{T}_1 and \hat{T}_2 , and filled circles represent the two-body interaction \hat{H}_2 . As before, the diagrams are implicitly antisymmetrized (Hugenholtz diagrams). Lines connected to \hat{T} are always directed upward because they represent an excitation operator while the directions of external lines connected to \hat{H}_2 are unconstrained.

CCSD amplitude equations become,

$$\begin{aligned} \langle \Phi_i^a | \left[\hat{H}_2 \left(\hat{T}_1 + \hat{T}_2 + \hat{T}_1 \hat{T}_2 + \frac{1}{2!} \hat{T}_1^2 + \frac{1}{3!} \hat{T}_1^3 \right) \right]_c | \Phi \rangle &= \varepsilon_i^a t_i^a \\ \langle \Phi_{ij}^{ab} | \left[\hat{H}_2 \left(1 + \hat{T}_1 + \hat{T}_2 + \frac{1}{2} \hat{T}_1^2 + \hat{T}_1 \hat{T}_2 + \frac{1}{2!} \hat{T}_2^2 + \frac{1}{3!} \hat{T}_1^3 + \frac{1}{2!} \hat{T}_1^2 \hat{T}_2 + \frac{1}{4!} \hat{T}_1^4 \right) \right]_c | \Phi \rangle &= \varepsilon_{ij}^{ab} t_{ij}^{ab} \end{aligned} \quad (3.12)$$

where ε are the Møller–Plesset denominators from Eq. (3.6). As usual, these non-linear equations are solved using an iterative procedure where the cluster amplitudes on the right-hand side of Eq. (3.12) are updated by calculating the terms on the left-hand side until a fixed point is reached. Like the HF iterative procedure, employing convergence acceleration techniques can reduce the number of CC iterations required.

$$E(\hat{T}, \hat{\Lambda}) = \langle \Phi | \hat{\Lambda} e^{-\hat{T}} \hat{H} e^{\hat{T}} | \Phi \rangle = \langle \Phi | \hat{\Lambda} \bar{H} | \Phi \rangle \quad (3.13)$$

$$\hat{\Lambda} \equiv \lambda_0 + \hat{\Lambda}_1 + \hat{\Lambda}_2 + \dots + \hat{\Lambda}_N \quad (3.14)$$

$$\hat{\Lambda}_k \equiv \left(\frac{1}{k!} \right)^2 \sum_{\substack{a_1 \dots a_k \\ i_1 \dots i_k}} \lambda_{a_1 \dots a_k}^{i_1 \dots i_k} \left\{ \hat{i}_1^\dagger \dots \hat{i}_k^\dagger \hat{a}_k \dots \hat{a}_1 \right\}, \quad (3.15)$$

$$\langle \Phi | \hat{\Lambda} \left[\bar{H}, \left\{ \hat{a}^\dagger \hat{i} \right\} \right] | \Phi \rangle = 0, \quad (3.16)$$

$$\langle \Phi | \hat{\Lambda} \left[\bar{H}, \left\{ \hat{a}^\dagger \hat{b}^\dagger \hat{j} \hat{i} \right\} \right] | \Phi \rangle = 0.$$

$$\langle \Phi | \hat{\Lambda} \bar{H} | \Phi_i^a \rangle = \omega \langle \Phi | \hat{\Lambda} | \Phi_i^a \rangle, \quad (3.17)$$

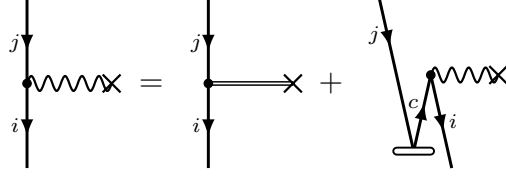
$$\langle \Phi | \hat{\Lambda} \bar{H} | \Phi_{ij}^{ab} \rangle = \omega \langle \Phi | \hat{\Lambda} | \Phi_{ij}^{ab} \rangle.$$

$$\begin{aligned}
\Delta E_{CCSD} &= \text{diagram 1} + \text{diagram 2} + \boxed{\text{diagram 3}} \\
&= \frac{1}{4} \sum_{klcd} V_{cd}^{kl} t_{kl}^{cd} + \frac{1}{2} \sum_{klcd} V_{cd}^{kl} t_k^c t_l^d + \boxed{\sum_{kc} f_c^k t_k^c}
\end{aligned} \tag{3.18}$$

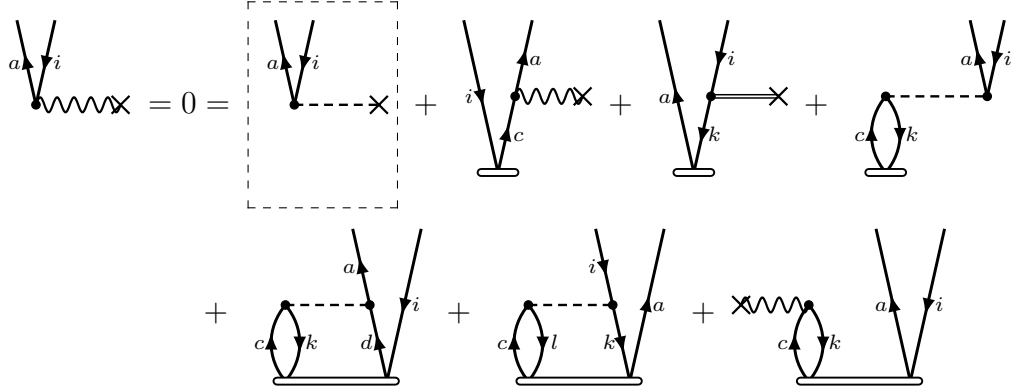
$$\begin{aligned}
\text{diagram 4} &= \boxed{\text{diagram 5}} + \text{diagram 6} \\
X_a^i &= \boxed{f_a^i} + \sum_{kc} V_{ac}^{ik} t_k^c
\end{aligned} \tag{3.19}$$

$$\begin{aligned}
\text{diagram 7} &= \text{diagram 8} + \text{diagram 9} + \text{diagram 10} + \text{diagram 11} \\
X_b^a &= f_b^a - \frac{1}{2} \sum_{klc} V_{bc}^{kl} t_{kl}^{ac} + \sum_{kc} V_{cb}^{ka} t_k^c - \sum_k X_b^k t_k^a
\end{aligned} \tag{3.20}$$

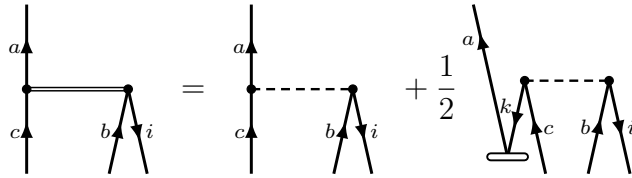
$$\begin{aligned}
\text{diagram 12} &= \text{diagram 13} + \text{diagram 14} + \text{diagram 15} \\
X_j^i &= f_j^i + \frac{1}{2} \sum_{kcd} V_{cd}^{ik} t_{jk}^{cd} + \sum_{kc} V_{jc}^{ik} t_k^c
\end{aligned} \tag{3.21}$$



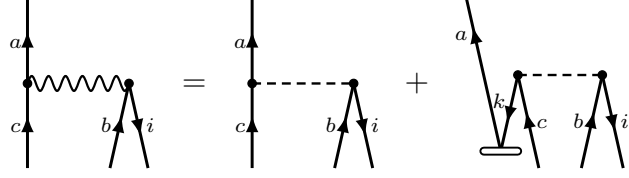
$$X_j^i = X_j'^i + \sum_c X_{ct_j}^{ic} \quad (3.22)$$



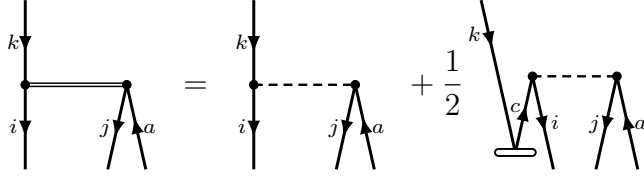
$$\begin{aligned} X_i^a = 0 &= \boxed{f_i^a} + \sum_c X_c^a t_i^c - \sum_k X_i'^k t_k^a + \sum_{kc} V_{ci}^{ka} t_k^c \\ &+ \frac{1}{2} \sum_{kcd} V_{cd}^{ka} t_{ki}^{cd} - \frac{1}{2} \sum_{klc} V_{ic}^{kl} t_{kl}^{ac} + \sum_{kc} X_c^k t_{ik}^{ac} \end{aligned} \quad (3.23)$$



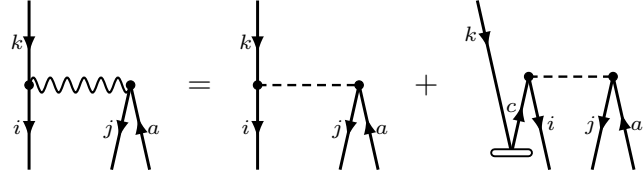
$$X_{bc}^{'ia} = V_{bc}^{ia} - \frac{1}{2} \sum_k V_{bc}^{ik} t_k^a \quad (3.24)$$



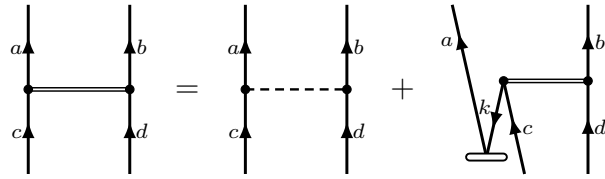
$$X_{bc}^{ia} = V_{bc}^{ia} - \sum_k V_{bc}^{ik} t_k^a \quad (3.25)$$



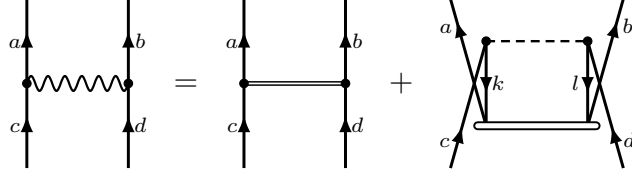
$$X_{ka}^{ij} = V_{ka}^{ij} + \frac{1}{2} \sum_c V_{ca}^{ij} t_k^c \quad (3.26)$$



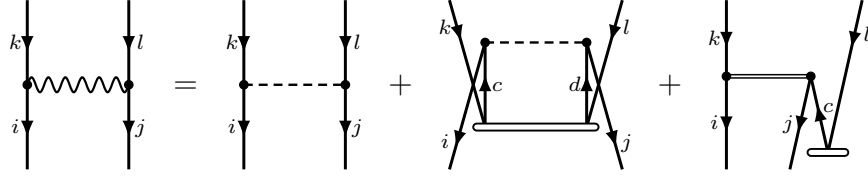
$$X_{ka}^{ij} = V_{ka}^{ij} + \sum_c V_{ca}^{ij} t_k^c \quad (3.27)$$



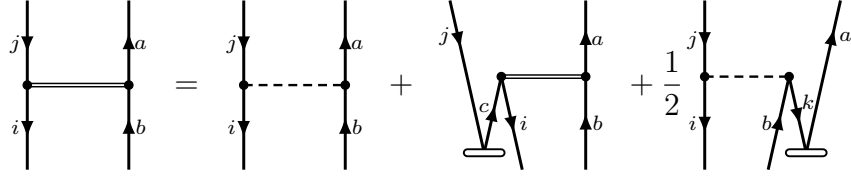
$$X_{cd}^{ab} = V_{cd}^{ab} - \hat{P}(ab) \sum_k X_{cd}^{kb} t_k^a \quad (3.28)$$



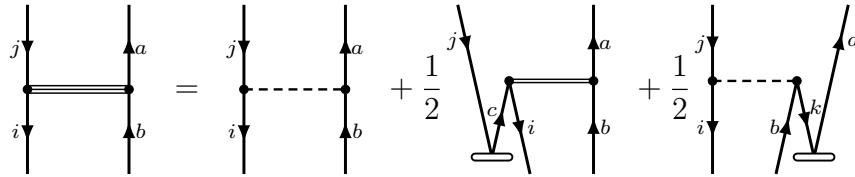
$$X_{cd}^{ab} = X_{cd}^{\prime ab} + \frac{1}{2} \sum_{kl} V_{cd}^{kl} t_{kl}^{ab} \quad (3.29)$$



$$X_{kl}^{ij} = V_{kl}^{ij} + \frac{1}{2} \sum_{cd} V_{cd}^{ij} t_{kl}^{cd} + \hat{P}(kl) \sum_c X_{kc}^{ij} t_l^c \quad (3.30)$$



$$X_{jb}^{\prime ia} = V_{jb}^{ia} + \sum_c X_{cb}^{\prime ia} t_j^c - \frac{1}{2} \sum_k V_{jb}^{ik} t_k^a \quad (3.31)$$

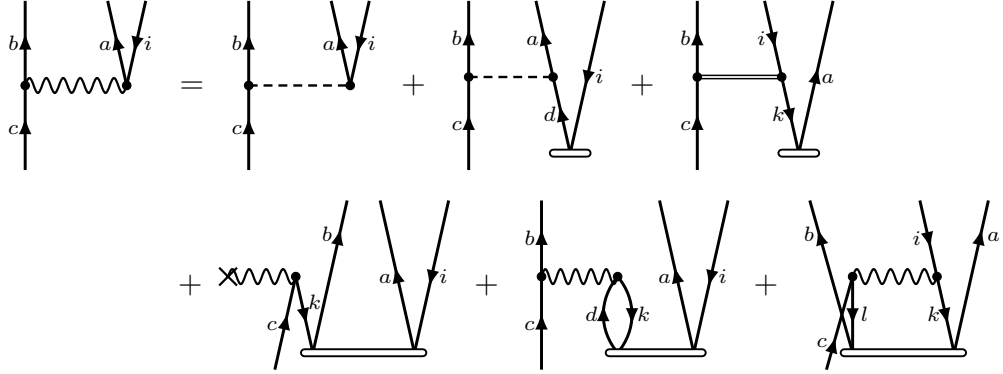


$$X_{jb}^{\prime\prime ia} = V_{jb}^{ia} + \frac{1}{2} \sum_c X_{cb}^{\prime ia} t_j^c - \frac{1}{2} \sum_k V_{jb}^{ik} t_k^a \quad (3.32)$$

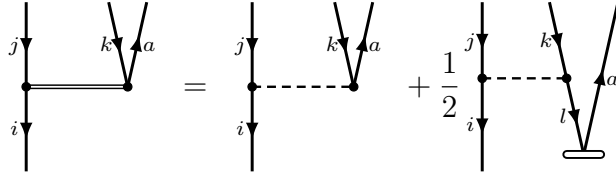
$$X'''_{jb}{}^{ia} = V_{jb}{}^{ia} + \frac{1}{2} \sum_c X_{cb}{}^{ia} t_j^c - \sum_k V_{jb}{}^{ik} t_k^a \quad (3.33)$$

$$X_{jb}{}^{ia} = X'''_{jb}{}^{ia} - \left(\frac{1}{2}\right) \sum_{kc} V_{cb}{}^{ik} t_{jk}^{ca} + \frac{1}{2} \sum_c X_{cb}{}^{ia} t_j^c \quad (3.34)$$

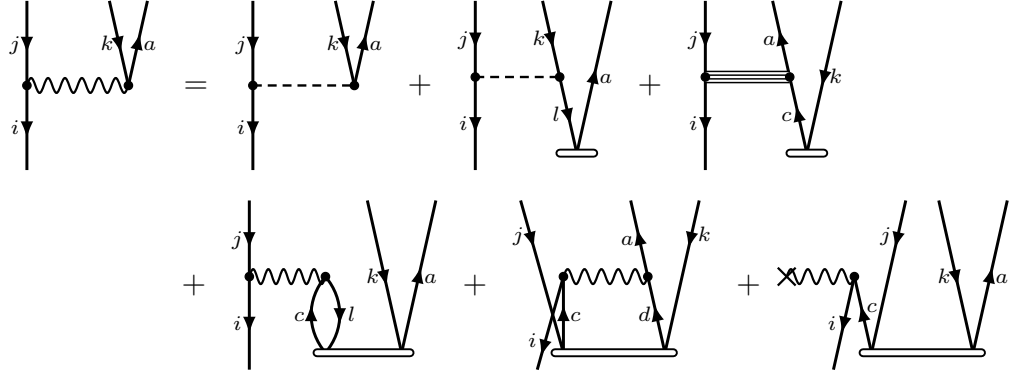
$$X'_{ic}{}^{ab} = V_{ic}{}^{ab} + \frac{1}{2} \sum_d V_{dc}{}^{ab} t_i^d - \hat{P}(ab) \sum_k X''_{ic}{}^{kb} t_k^a \quad (3.35)$$



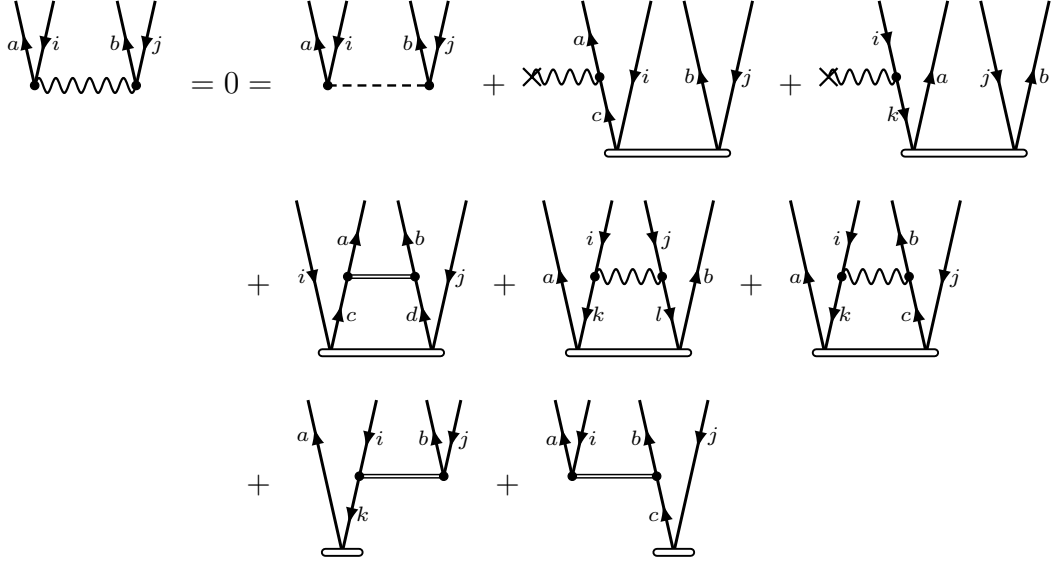
$$\begin{aligned}
X_{ic}^{ab} &= V_{ic}^{ab} + \sum_d V_{dc}^{ab} t_i^d - \hat{P}(ab) \sum_k X_{ic}^{'kb} t_k^a \\
&\quad - \sum_k X_c^k t_{ik}^{ab} + \hat{P}(ab) \sum_{kd} X_{dc}^{kb} t_{ik}^{ad} + \frac{1}{2} \sum_{kl} X_{ic}^{kl} t_{kl}^{ab}
\end{aligned} \tag{3.36}$$



$$X_{jk}^{'ia} = V_{jk}^{ia} - \frac{1}{2} \sum_l V_{jk}^{il} t_l^a \tag{3.37}$$



$$\begin{aligned}
X_{jk}^{ia} &= V_{jk}^{ia} - \sum_l V_{jk}^{il} t_l^a + \hat{P}(jk) \sum_c X_{jc}^{iia} t_k^c \\
&+ \hat{P}(jk) \sum_{lc} X_{jc}^{il} t_{lk}^{ca} + \frac{1}{2} \sum_{cd} X_{cd}^{ia} t_{jk}^{cd} + \sum_c X_c^{i} t_{jk}^{ca}
\end{aligned} \tag{3.38}$$



$$\begin{aligned}
X_{ij}^{ab} = 0 = & V_{ij}^{ab} + \hat{P}(ab) \sum_c X_c^a t_{ij}^{cb} - \hat{P}(ij) \sum_k X_i^k t_{kj}^{ab} \\
& + \frac{1}{2} \sum_{cd} X_{cd}^{ab} t_{ij}^{cd} + \frac{1}{2} \sum_{kl} X_{ij}^{kl} t_{kl}^{ab} - \hat{P}(ab|ij) \sum_{kc} X_{ic}^{kb} t_{kj}^{ac} \\
& - \hat{P}(ab) \sum_k X_{ij}^{kb} t_k^a + \hat{P}(ij) \sum_c X_{ic}^{ab} t_j^c
\end{aligned} \tag{3.39}$$

$$\begin{aligned}
0 = & \text{Diagram 1} + \text{Diagram 2} + \text{Diagram 3} + \text{Diagram 4} + \text{Diagram 5} \\
& + \text{Diagram 6} + \text{Diagram 7} + \text{Diagram 8} \\
= & X_a^i + \sum_c \lambda_c^i X_a^c - \sum_k \lambda_a^k X_k^i + \sum_{kc} \lambda_c^k X_{ak}^{ic} + \frac{1}{2} \sum_{kcd} \lambda_{cd}^{ik} X_{ak}^{cd} \\
& - \frac{1}{2} \sum_{klc} \lambda_{ac}^{kl} X_{kl}^{ic} - \frac{1}{2} \sum_{jklcd} \lambda_{cd}^{jl} X_{aj}^{ik} t_{kl}^{cd} + \frac{1}{2} \sum_{klbcd} \lambda_{bc}^{kl} X_{ad}^{ic} t_{kl}^{bd}
\end{aligned} \tag{3.40}$$

$$\begin{aligned}
& = X_a^i + \sum_c \lambda_c^i X_a^c - \sum_k \lambda_a^k X_k^i - \sum_{kc} \lambda_c^k X_{ka}^{ic} - \frac{1}{2} \sum_{kcd} \lambda_{cd}^{ik} X_{ka}^{cd} \\
& - \frac{1}{2} \sum_{klc} \lambda_{ac}^{kl} X_{kl}^{ic} + \frac{1}{2} \sum_{jklcd} \lambda_{cd}^{jl} X_{ja}^{ik} t_{kl}^{cd} - \frac{1}{2} \sum_{klbcd} \lambda_{cb}^{kl} X_{ad}^{ic} t_{kl}^{bd} \\
& = X_a^i + \lambda_c^i X_a^c - X_k^i \lambda_a^k - X_{k\bar{c}}^{i\bar{a}} \lambda^{k\bar{c}} - \frac{1}{2} \lambda_{cd\bar{k}}^i X_a^{cd\bar{k}} \\
& - \frac{1}{2} X_{kl\bar{c}}^i \lambda_a^{kl\bar{c}} + \frac{1}{2} X_{j\bar{k}}^{i\bar{a}} \left(\lambda_{cd\bar{l}}^j t_k^{cd\bar{l}} \right)^{j\bar{k}} - \frac{1}{2} X_{d\bar{c}}^{i\bar{a}} \left(t_{kl\bar{b}}^d \lambda_c^{kl\bar{b}} \right)^{d\bar{c}}
\end{aligned}$$

$$\begin{aligned}
\lambda_3 & \leftarrow X_{\text{hp}3} + \lambda_3 X_{\text{pp}3} - X_{\text{hh}3} \lambda_3 - \frac{1}{2} \lambda_{31} X_{\text{pphp}34} - \frac{1}{2} X_{\text{hphh}31} \lambda_{33} \\
\lambda_2 & \leftarrow -X_{\text{hphp}21} \lambda_2 + \frac{1}{2} X_{\text{hhhp}21} \left(\lambda_{31} t_{33} \right)_2 - \frac{1}{2} X_{\text{hppp}23} \left(t_{32} \lambda_{33} \right)_2
\end{aligned}$$

$$\begin{aligned}
0 = & \text{Diagram 1} + \text{Diagram 2} + \text{Diagram 3} + \text{Diagram 4} \\
& + \text{Diagram 5} + \text{Diagram 6} + \text{Diagram 7} + \text{Diagram 8} \\
& + \text{Diagram 9} + \text{Diagram 10} + \text{Diagram 11} \\
= & V_{ab}^{ij} + \hat{P}(ab|ij) \lambda_a^i X_b^j - \hat{P}(ab) \sum_k \lambda_a^k X_{kb}^{ij} + \hat{P}(ij) \sum_c \lambda_c^i X_{ab}^{cj} \\
& + \hat{P}(ab) \sum_c \lambda_{ac}^{ij} X_b^c - \hat{P}(ij) \sum_k \lambda_{ab}^{ik} X_k^j + \frac{1}{2} \sum_{cd} \lambda_{cd}^{ij} X_{ab}^{cd} + \frac{1}{2} \sum_{kl} \lambda_{ab}^{kl} X_{kl}^{ij} \\
& - \hat{P}(ab|ij) \sum_{kc} \lambda_{ac}^{kj} X_{kb}^{ic} - \hat{P}(ab) \frac{1}{2} \sum_{klcd} \lambda_{ad}^{kl} V_{cb}^{ij} t_{kl}^{cd} - \hat{P}(ij) \frac{1}{2} \sum_{klcd} \lambda_{cd}^{il} V_{ab}^{kj} t_{kl}^{cd} \quad (3.41)
\end{aligned}$$

$$\begin{aligned}
&= V_{ab}^{ij} + \hat{P}(ab|ij) \lambda_a^i X_b^j - \hat{P}(ab) \sum_k \lambda_a^k X_{kb}^{ij} - \hat{P}(ij) \sum_c \lambda_c^i X_{ab}^{jc} \\
&\quad - \hat{P}(ab) \sum_c \lambda_{ca}^{ij} X_b^c + \hat{P}(ij) \sum_k \lambda_{ab}^{ki} X_k^j + \frac{1}{2} \sum_{cd} \lambda_{cd}^{ij} X_{ab}^{cd} + \frac{1}{2} \sum_{kl} \lambda_{ab}^{kl} X_{kl}^{ij} \\
&\quad - \hat{P}(ab|ij) \sum_{kc} \lambda_{ac}^{kj} X_{kb}^{ic} - \hat{P}(ab) \frac{1}{2} \sum_{klcd} \lambda_{ad}^{kl} V_{cb}^{ij} t_{kl}^{cd} - \hat{P}(ij) \frac{1}{2} \sum_{klcd} \lambda_{cd}^{il} V_{ab}^{kj} t_{kl}^{cd} \\
&= V_{ab}^{ij} + \hat{P}(ab|ij) \left(\lambda_a^i X_b^j \right)_{ab}^{ij} - \hat{P}(ab) X_k^{ij\bar{b}} \lambda_a^k - \hat{P}(ij) \lambda_c^i X_{ab\bar{j}}^c \\
&\quad - \hat{P}(ab) \lambda_c^{ij\bar{a}} X_b^c + \hat{P}(ij) X_k^j \lambda_{ab\bar{i}}^k + \frac{1}{2} \lambda_{cd}^{ij} X_{ab}^{cd} + \frac{1}{2} X_{kl}^{ij} \lambda_{ab}^{kl} \\
&\quad - \hat{P}(ab|ij) X_{k\bar{c}}^{i\bar{b}} \lambda_{a\bar{j}}^{k\bar{c}} - \hat{P}(ab) \frac{1}{2} V_c^{ij\bar{b}} \left(t_{k\bar{l}\bar{d}}^c \lambda_a^{kl\bar{d}} \right) - \hat{P}(ij) \frac{1}{2} \left(\lambda_{cd\bar{l}}^i t_k^{cd\bar{l}} \right) V_{ab\bar{j}}^k
\end{aligned} \tag{3.42}$$

$$\begin{aligned}
\lambda_1 &\leftarrow V_{hhpp1} + \hat{P}(\lambda_3 X_{hp3})_1 + \frac{1}{2} \lambda_1 X_{pppp1} + \frac{1}{2} X_{hhhh1} \lambda_1 \\
\lambda_{33(4)} &\leftarrow -(+) X_{hhhp33} \lambda_3 + (-) \lambda_{33} X_{pp3} - (+) \frac{1}{2} V_{hhpp33} (t_{31} \lambda_{33}) \\
\lambda_{31(2)} &\leftarrow -(+) \lambda_3 X_{hppp32} - (+) X_{hh3} \lambda_{31} - (+) \frac{1}{2} (\lambda_{31} t_{33}) V_{hhpp31} \\
\lambda_{21(2)} &\leftarrow -X_{hphp21} \lambda_{21} \\
\lambda_{23(4)} &\leftarrow X_{hphp21} \lambda_{21}
\end{aligned}$$

Chapter 4

Equation-of-Motion Method

$$\hat{H} = H_{\emptyset} + \sum_{pq} H_{pq} \left\{ \hat{a}_p^\dagger \hat{a}_q \right\} + \frac{1}{4} \sum_{pqrs} H_{pqrs} \left\{ \hat{a}_p^\dagger \hat{a}_q^\dagger \hat{a}_s \hat{a}_r \right\}, \quad (4.1)$$

Particle attached and particle removed equations-of-motion (EOM) methods can be coupled with either IM-SRG or CC calculations. The principal idea is that one may construct a ladder operator \hat{X} that promotes the N -particle ground state to any state in the $N + 1$ or $N - 1$ spectrum,

$$|\Psi_u^{(N\pm 1)}\rangle = \hat{X}_u^{(N\pm 1)} |\Psi_0^{(N)}\rangle, \quad (4.2)$$

where \hat{X} is in principle a linear combination of excitation (+) and de-excitation (−) operators that change particle number by one,

$$\hat{X}_u^{(N+1)} = \sum_a x_a^{(u,+)} \left\{ \hat{a}_a^\dagger \right\} + \frac{1}{2} \sum_{abi} x_{abi}^{(u,+)} \left\{ \hat{a}_a^\dagger \hat{a}_b^\dagger \hat{a}_i \right\} + \dots, \quad (4.3)$$

$$\hat{X}_u^{(N-1)} = \sum_i x_i^{(u,-)} \left\{ \hat{a}_i \right\} + \frac{1}{2} \sum_{ija} x_{ija}^{(u,-)} \left\{ \hat{a}_a^\dagger \hat{a}_j \hat{a}_i \right\} + \dots. \quad (4.4)$$

Here, $x_p^{(u,\pm)}$ and $x_{pqr}^{(u,\pm)}$ are the normal-ordered matrix elements of $\hat{X}_u^{(N\pm 1)}$, defined analogously to Eq. (4.1).

Substitution of Eq. (4.2) into the energy eigenvalue problem

$$\hat{H} |\Psi_u^{(N\pm 1)}\rangle = E_u^{(N\pm 1)} |\Psi_u^{(N\pm 1)}\rangle,$$

gives

$$[\hat{H}, \hat{X}_u^{(N\pm 1)}]|\Psi_0^{(N)}\rangle = \pm \varepsilon_u^{(\pm)} \hat{X}_u^{(N\pm 1)}|\Psi_0^{(N)}\rangle, \quad (4.5)$$

which constitutes a generalized eigenvalue problem for the amplitudes x , where $\varepsilon_u^{(\pm)}$ are the single-particle addition (+) and removal (−) energies. The quality of this calculation depends on the ansatz for the N -particle ground state, as well as the systematically improvable truncation on the ladder operators. In this work we include 1p and 2p1h excitations in the $N + 1$ ladder operator and likewise 1h and 2h1p operators for the $N - 1$ ladder operators.

After a single-reference ground state IM-SRG calculation, the Hamiltonian has been rotated such that the reference state is an eigenfunction with corresponding eigenvalue $E_0^{(N)}$, which is the correlated N -particle ground state energy. The EOM equation is therefore

$$[\bar{H}, \bar{X}_u^{(N\pm 1)}]|\Phi_0^{(N)}\rangle = \pm \varepsilon_u^{(\pm)} \bar{X}_u^{(N\pm 1)}|\Phi_0^{(N)}\rangle, \quad (4.6)$$

where bars denote rotated operators. Now the reference state is used in place of the bare correlated ground state. The ground state IM-SRG procedure has implicitly re-summed contributions from higher order excitations (3-particle-2-hole, 2-particle-3-hole, 2-particle-3-hole, 4-particle-3-hole, ...) into the lower order amplitudes of the ladder operators (1-particle-0-hole, 0-particle-1-hole, 2-particle-1-hole, 1-particle-2-hole).

Despite these gains, the EOM calculation is still a partial diagonalization method, limited by the truncation to 2-particle-1-hole and 1-particle-2-hole operators. We expect $N + 1$ (or $N - 1$) states to be described appropriately by EOM-IM-SRG if their wavefunctions are dominated by 1-particle-0-hole (or 0-particle-1-hole) contributions in the rotated frame. We

use partial norms of the EOM ladder operators to estimate these contributions:

$$n_{1\text{-particle}} = \sqrt{\sum_a |\bar{x}_a^{(+)}|^2}, \quad (4.7)$$

$$n_{1\text{-hole}} = \sqrt{\sum_i |\bar{x}_i^{(-)}|^2}. \quad (4.8)$$

Large single particle partial norms indicate that the EOM truncation is reasonable for the relevant state. States with lower single particle norms should be treated with a higher EOM approximation, which can be accomplished directly or perturbatively [54].

Like EOM-IM-SRG, the equations-of-motion technique can be applied after a CC ground-state calculation, by using the CC effective Hamiltonian. Here, the non-Hermitian nature of \bar{H}_{CC} becomes apparent. In this case, in addition to constructing excitation ladder operators Eq. (4.3) and Eq. (4.4) that correspond to the right-eigenvectors of the generalized eigenvalue problem Eq. (4.6), there exist analogous de-excitation ladder operators, $\hat{L}^{(N+1)}$ and $\hat{L}^{(N-1)}$, that correspond to the left-eigenvectors,

$$\begin{aligned} \hat{L}_u^{(N+1)} &= \sum_a l_a^{(u,+)} \{\hat{a}_a\} + \frac{1}{2} \sum_{iab} l_{iab}^{(u,+)} \{\hat{a}_i^\dagger \hat{a}_b \hat{a}_a\} + \dots, \\ \hat{L}_u^{(N-1)} &= \sum_i l_i^{(u,-)} \{\hat{a}_i^\dagger\} + \frac{1}{2} \sum_{ija} l_{ija}^{(u,-)} \{\hat{a}_i^\dagger \hat{a}_j^\dagger \hat{a}_a\} + \dots, \end{aligned}$$

where $l_p^{(u,\pm)}$ and $l_{pqr}^{(u,\pm)}$ are likewise the normal-ordered matrix elements of $\hat{L}_u^{(N\pm 1)}$. These left-eigenvectors satisfy the left-eigenvalue problem, with left-eigenvalues $\varepsilon_u^{(\pm)}$, analogous to Eq. (4.6),

$$\langle \Phi_0^{(N)} | [\bar{H}, \bar{L}_u^{(N\pm 1)}] = \pm \varepsilon_u^{(\pm)} \langle \Phi_0^{(N)} | \bar{L}_u^{(N\pm 1)}$$

and form a bi-orthogonal set with the right-eigenvectors, $\langle \bar{L}_u^{(N\pm 1)} | \bar{X}_v^{(N\pm 1)} \rangle = \delta_{uv}$.

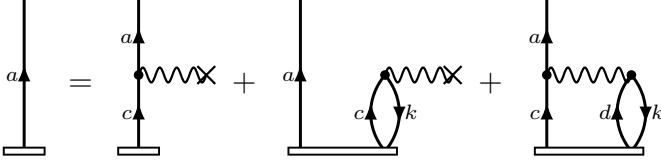
In this paper, because the effective Hamiltonian is real, the corresponding left- and right-eigenvalues are equal. In addition, while the the left- and right-eigenvectors are generally not equivalent, the differences in their single-particle Eq. (4.7) or single-hole Eq. (4.8) natures are, in practice, not significant. Therefore, only the right-eigenvectors are used in this paper.

$$\langle \Phi_0 | \hat{L}_\nu^{+1} \bar{H}_N \hat{R}_\nu^{+1} | \Phi_0 \rangle_c =$$

$$+ \quad (4.9)$$

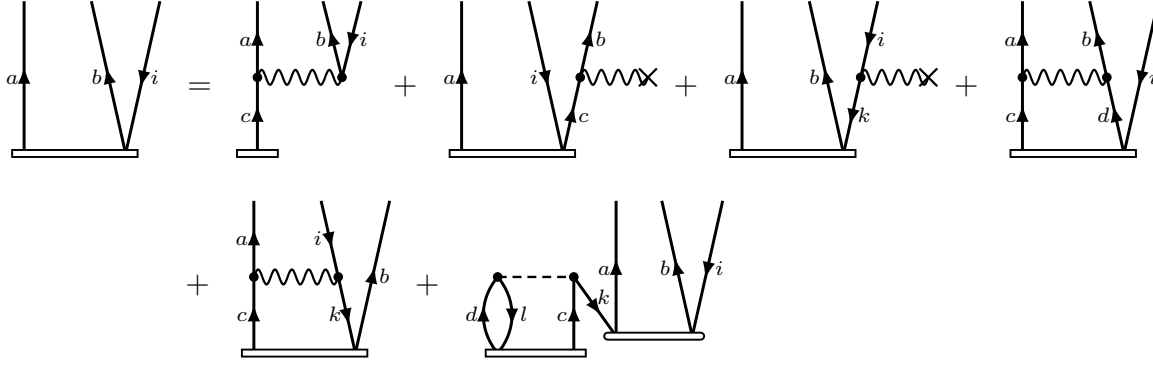
$$\langle \Phi_0 | \hat{L}_\nu^{-1} \bar{H}_N \hat{R}_\nu^{-1} | \Phi_0 \rangle_c =$$

$$+ \quad (4.10)$$



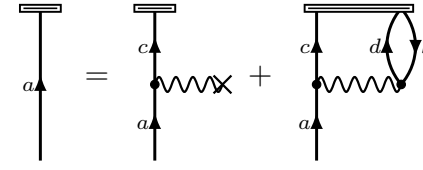
$$\omega_k r^a = \sum_c X_c^a r^c + \sum_{kc} X_c^k r_k^{ac} + \frac{1}{2} \sum_{kcd} X_{cd}^{ak} r_k^{cd} \quad (4.11)$$

$$\begin{aligned} \omega_k r^a &= \sum_c X_c^a r^c + \sum_{kc} X_c^k r_k^{ac} - \frac{1}{2} \sum_{kcd} X_{cd}^{ka} r_k^{cd} \\ \omega_k r^a &= X_c^a r^c + r_{k\bar{c}}^a X^{k\bar{c}} - \frac{1}{2} X_{cd\bar{k}}^a r^{cd\bar{k}} \\ \omega_k r &\leftarrow X_{\text{pp}3} r + r_{21} X_{\text{hp}2} - \frac{1}{2} X_{\text{hppp}3_2} r_{3_4} \end{aligned} \quad (4.12)$$



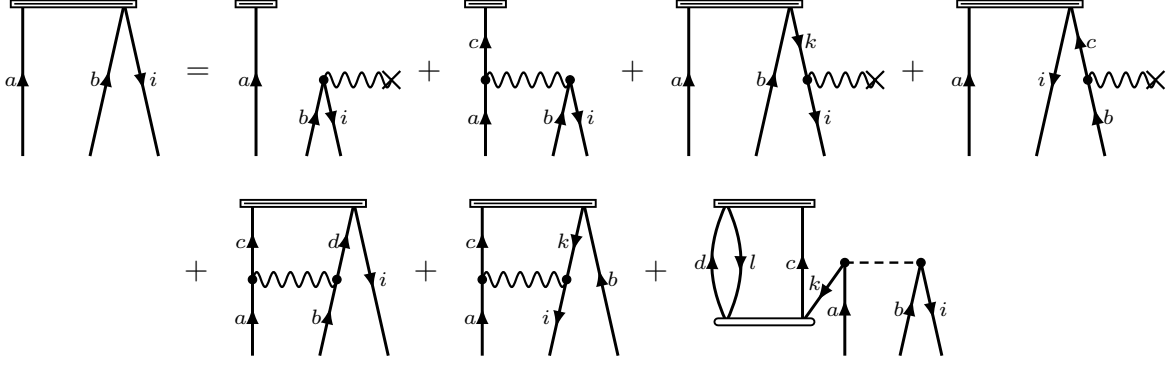
$$\begin{aligned} \omega_k r_i^{ab} &= \sum_c X_{ci}^{ab} r^c + \hat{P}(ab) \sum_c X_c^b r_i^{ac} - \sum_k X_i^k r_k^{ab} + \frac{1}{2} \sum_{cd} X_{cd}^{ab} r_i^{cd} \\ &\quad - \hat{P}(ab) \sum_{kc} X_{ci}^{ak} r_k^{cb} - \frac{1}{2} \sum_{klcd} V_{cd}^{kl} t_{ki}^{ab} r_l^{cd} \end{aligned} \quad (4.13)$$

$$\begin{aligned}
\omega_k r_i^{ab} &= -\sum_c X_{ic}^{ab} r^c + \hat{P}(ab) \sum_c X_c^b r_i^{ac} - \sum_k X_i^k r_k^{ab} + \frac{1}{2} \sum_{cd} X_{cd}^{ab} r_i^{cd} \\
&\quad - \hat{P}(ab) \sum_{kc} X_{ic}^{ka} r_k^{cb} - \frac{1}{2} \sum_{klcd} V_{cd}^{kl} t_{ki}^{ab} r_l^{cd} \\
\omega_k r_i^{ab} &= -X_c^{ab\bar{i}} r^c + \hat{P}(ab) X_c^b r_{i\bar{a}}^c - r_k^{ab} X_i^k + \frac{1}{2} X_{cd}^{ab} r_i^{cd} \\
&\quad - \hat{P}(ab) r_{k\bar{c}}^b X_{i\bar{a}}^{k\bar{c}} - \frac{1}{2} t_k^{ab\bar{i}} V_{cd\bar{l}}^k r^{cd\bar{l}} \\
\omega_k r_3 &\leftarrow -X_{\text{pphp}3_4} r - \frac{1}{2} t_{3_3} V_{\text{hhpp}3_1} r_{3_3} \\
\omega_k r_{3_2} &\leftarrow X_{\text{pp}3} r_{3_2} - r_{3_2} X_{\text{hphp}2_1} \\
\omega_k r_{3_1} &\leftarrow -X_{\text{pp}3} r_{3_2} + r_{3_2} X_{\text{hphp}2_1} \\
\omega_k r_1 &\leftarrow -r_1 X_{\text{hh}3} + \frac{1}{2} X_{\text{pppp}1} r_1
\end{aligned} \tag{4.14}$$



$$E_k l_a = \sum_c l_c X_a^c + \frac{1}{2} \sum_{kcd} l_{cd}^k X_{ak}^{cd} \tag{4.15}$$

$$\begin{aligned}
E_k l_a &= \sum_c l_c X_a^c - \frac{1}{2} \sum_{kcd} l_{cd}^k X_{ka}^{cd} \\
E_k l_a &= l_c X_a^c - \frac{1}{2} l_{cd\bar{k}} X_a^{cd\bar{k}} \\
E_k l &\leftarrow l X_{\text{pp}3} - \frac{1}{2} l_3 X_{\text{pphp}3_4}
\end{aligned} \tag{4.16}$$



$$\begin{aligned}
E_k l_{ab}^i &= \hat{P}(ab) l_a X_b^i + \sum_c l_c X_{ab}^{ci} - \sum_k l_{ab}^k X_k^i + \hat{P}(ab) \sum_c l_{ac}^i X_b^c \\
&+ \frac{1}{2} \sum_{cd} l_{cd}^i X_{ab}^{cd} - \hat{P}(ab) \sum_{kc} l_{cb}^k X_{ak}^{ci} - \frac{1}{2} \sum_{klcd} l_{cd}^l V_{ab}^{ki} t_{kl}^{cd}
\end{aligned} \tag{4.17}$$

$$\begin{aligned}
E_k l_{ab}^i &= \hat{P}(ab) l_a X_b^i - \sum_c l_c X_{ab}^{ic} - \sum_k l_{ab}^k X_k^i + \hat{P}(ab) \sum_c l_{ac}^i X_b^c \\
&+ \frac{1}{2} \sum_{cd} l_{cd}^i X_{ab}^{cd} - \hat{P}(ab) \sum_{kc} l_{cb}^k X_{ka}^{ic} - \frac{1}{2} \sum_{klcd} l_{cd}^l V_{ab}^{ki} t_{kl}^{cd}
\end{aligned}$$

$$\begin{aligned}
E_k l_{ab}^i &= \hat{P}(ab) l_a X_b^{i\bar{b}} - l_c X_{abi}^c - X_k^i l_{ab}^k + \hat{P}(ab) l_c^{i\bar{a}} X_b^c \\
&+ \frac{1}{2} l_{cd}^i X_{ab}^{cd} - \hat{P}(ab) X_{kc}^{i\bar{a}} l_{ab}^{k\bar{c}} - \frac{1}{2} l_{cd}^l t_k^{cd\bar{l}} V_{abi}^k
\end{aligned}$$

$$E_k l_3 \leftarrow -l X_{\text{hppp}3_2} - \frac{1}{2} l_3 t_{3_3} V_{\text{hphp}3_1}$$

$$E_k l_{3_2} \leftarrow -l X_{\text{hp}2} + l_{3_2} X_{\text{pp}3} - X_{\text{hphp}2_1} l_{3_2}$$

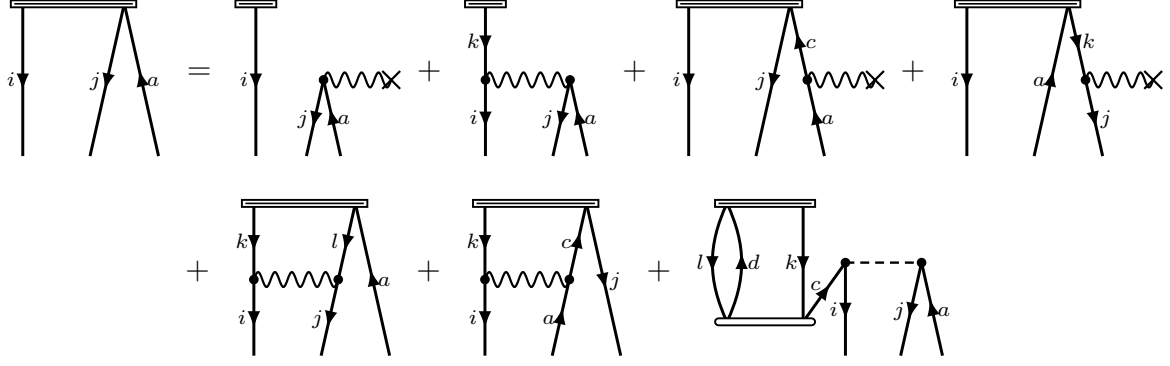
$$E_k l_{3_1} \leftarrow l X_{\text{hp}2} - l_{3_2} X_{\text{pp}3} + X_{\text{hphp}2_1} l_{3_2}$$

$$E_k l_1 \leftarrow -X_{\text{hh}3} r_1 + \frac{1}{2} l_1 X_{\text{pppp}1} \tag{4.18}$$

$$\omega_k r_i = - \sum_k X_i^k r_k + \sum_{kc} X_c^k r_{ik} - \frac{1}{2} \sum_{klc} X_{ic}^{kl} r_{kl} \quad (4.19)$$

$$\begin{aligned} \omega_k r_{ij}^a = & - \sum_k X_{ij}^{ka} r_k - \hat{P}(ij) \sum_k X_j^k r_{ik}^a + \sum_c X_c^a r_{ij}^c + \frac{1}{2} \sum_{kl} X_{ij}^{kl} r_{kl}^a \\ & - \hat{P}(ij) \sum_{kc} X_{ci}^{ak} r_{kj}^c - \frac{1}{2} \sum_{klcd} V_{cd}^{kl} t_{ij}^{ca} r_{kl}^d \end{aligned} \quad (4.20)$$

$$E_k l^i = - \sum_k l^k X_k^i - \frac{1}{2} \sum_{klc} l_c^{kl} X_{kl}^{ic} \quad (4.21)$$



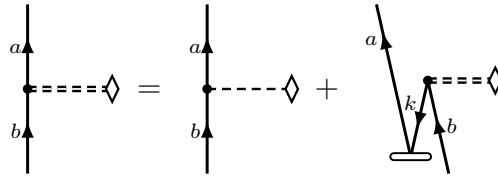
$$\begin{aligned}
E_k l_a^{ij} &= \hat{P}(ij) l^i X_a^j - \sum_k l^k X_{ka}^{ij} + \sum_c l_c^{ij} X_a^c - \hat{P}(ij) \sum_k l_a^{ik} X_k^j \\
&+ \frac{1}{2} \sum_{cd} l_a^{kl} X_{kl}^{ij} - \hat{P}(ij) \sum_{kc} l_c^{kj} X_{ak}^{ci} - \frac{1}{2} \sum_{klcd} l_d^{kl} V_{ca}^{ij} t_{kl}^{cd}
\end{aligned} \tag{4.22}$$

Chapter 5

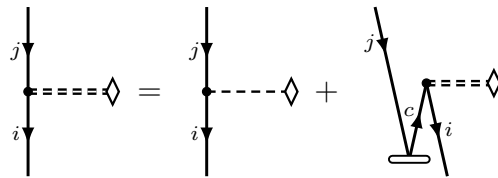
Effective Operators



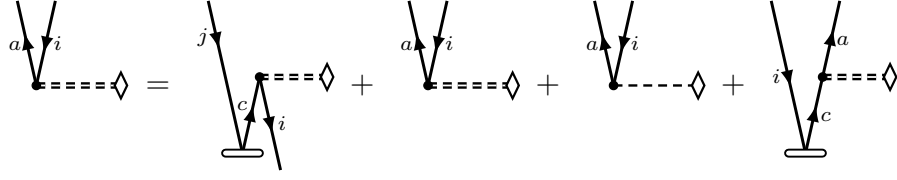
$$\lambda \bar{O}_a^i = \lambda O_a^i \quad (5.1)$$



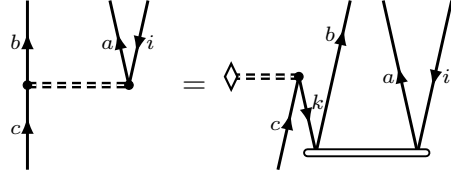
$$\lambda \bar{O}_b^a = \lambda O_b^a - \sum_k \lambda \bar{O}_b^k t_k^a \quad (5.2)$$



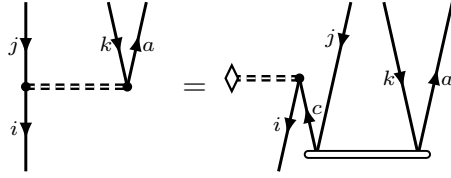
$$\lambda \bar{O}_j^i = \lambda O_j^i + \sum_c \lambda \bar{O}_c^i t_j^c \quad (5.3)$$



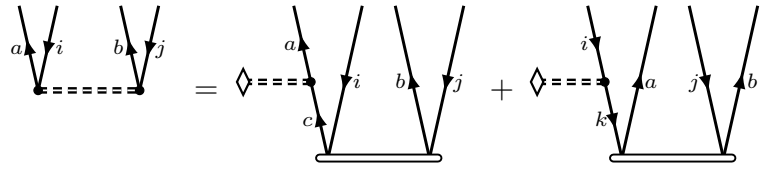
$$\lambda \bar{O}_i^a = \lambda O_i^a + \sum_c \lambda \bar{O}_c^a t_i^c - \sum_k \lambda \bar{O}_i^k t_k^a + \sum_{kc} \lambda \bar{O}_c^k t_{ik}^{ac} \quad (5.4)$$



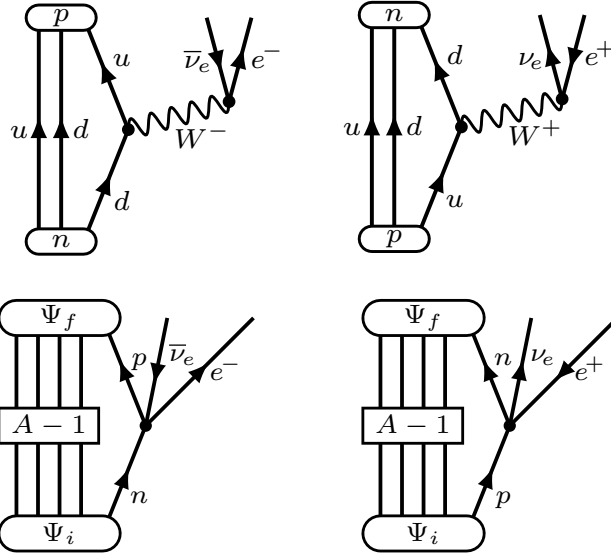
$$\lambda \bar{O}_{ic}^{ab} = - \sum_k \lambda \bar{O}_c^k t_{ik}^{ab} \quad (5.5)$$



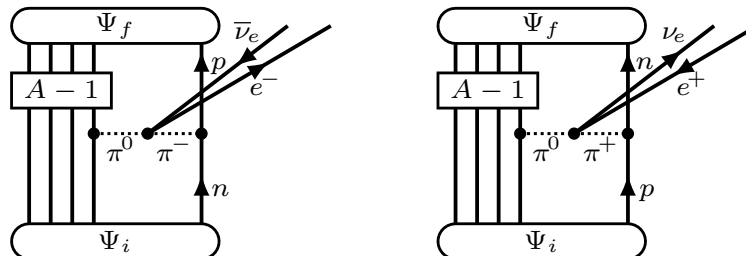
$$\lambda \bar{O}_{jk}^{ia} = \sum_c \lambda \bar{O}_c^i t_{jk}^{ca} \quad (5.6)$$



$$\lambda \bar{O}_{ij}^{ab} = \hat{P}(ab) \sum_c \lambda \bar{O}_c^a t_{ij}^{cb} - \hat{P}(ij) \sum_k \lambda \bar{O}_i^k t_{kj}^{ab} \quad (5.7)$$



5.1 Beta Decay



Chapter 6

Conclusions and Perspectives

Chapter 7

Instructions

If you want to use this class, it's probably a good idea to use the source code of this example document as a starting point.

7.1 Preamble

The document class may be declared using `\documentclass[<type>]{msudissertation}`, where `<type>` is either `dissertation` (default) or `thesis`. The class is based on the `book` class and thus inherits all its structural conventions. The WikiBooks has more information about this: https://en.wikibooks.org/wiki/LaTeX/Document_Structure .

Afterward, you can load your packages. Among those, you may find the following packages useful:

- `\usepackage{hyperref}`: provides hyperlinks (`\url`) and PDF bookmarks
- `\usepackage{pdflscape}`: provides `\begin{landscape} ... \end{landscape}`
- `\usepackage{titling}`: provides `\thetitle`, `\theauthor`, and `\thedata`

Refer to their official documentation on CTAN for more details.

To set the title, author, degree program, and date, include the following commands in your preamble:

- `\title{<title>}`

- `\author{<name>}`
- `\def\thedegreeprogram{<subject>---<degree>}`
- `\date{<year>}` (optional) Per university guidelines, the date must be contain only a 4-digit year. If omitted, it defaults to the current year, which could be undesirable if you want the reproduce the document years later.

The rest of the document is divided into three major parts, preceded the special markers `\frontmatter`, `\mainmatter`, and `\appendix` respectively.

7.2 Front matter

In the front matter, certain chapter names have been endowed with special meanings, e.g. `\chapter{Abstract}` or `\chapter{Copyright}`. This is what allows them to have unique formatting. They must be spelled and capitalized exactly as written in the source code of this example, unless otherwise specified. Given that the `\chapter` command has been imbued with some rather fragile (read: hacky) logic, try not to sneeze on them too hard.

The front matter in this example is a lot more packed than your typical dissertation or thesis, because a lot of the chapters are optional and have been filled with placeholder text. They can be safely deleted if neither you nor the university guidelines require them.

7.3 Main matter

The main matter is the most uninteresting part of this template, because it's almost the same as your vanilla book class. Just write `\chapter{<chapter>}` and `\section{<section>}` like you normally do.

Chapter 8

Appendix

You can have as many appendices as you want, or none at all. If you do have *at least one*, use the `\appendix` macro to create a cover page with the correct grammatical number depending on how many you have, and adjusts the table of contents according to university guidelines. After this macro, all uses of `\chapter{<chapter>}` will create an appendix chapter instead of a regular chapter. Do *not* use `\appendix` if you have no appendices at all.

At the very end, there is the mandatory bibliography. Here, I’m assuming you want to use the traditional `natbib`. If so, start by selecting a `\bibliographystyle{<style>}`. If you don’t like calling it “Bibliography”, you can pick a more suitable title using the syntax `\renewcommand{\bibname}{<title>}` as long as it conforms to university guidelines. Afterward, you can write `\bibliography{<name>}` where `<name>` is the path to the `.bib` database without the file extension.

And that’s it! The remaining part of this document is full of placeholder text so you can stop reading now.

Chapter 9

Lorem ipsum

Lorem ipsum dolor sit amet, consectetur adipiscing elit. Ut et leo non tortor viverra sodales. Ut condimentum odio orci, a varius sapien vehicula quis. Pellentesque a lacus sed sem gravida scelerisque. Nunc rutrum ornare fringilla. Donec ac lorem non leo tincidunt finibus quis in lectus.[25]

Pellentesque ac consequat leo. Nulla vel aliquet ex. Nulla non faucibus sapien, eu port-titor ligula:

$$I = \int_{-\infty}^{\infty} \frac{x}{1 + e^{-x^2/2}} dx \quad (9.1)$$

Class aptent taciti sociosqu ad litora torquent per conubia nostra, per inceptos himenaeos. In odio metus, maximus sed dictum vel, rhoncus id ante. Phasellus viverra sodales neque ut pulvinar.

Sed neque metus, elementum at risus in, imperdiet iaculis dolor. Vivamus quis libero quis dui finibus imperdiet. Nunc mollis odio eget nibh volutpat interdum. Praesent non felis in sem luctus gravida.

9.1 Pellentesque Scelerisque

Pellentesque scelerisque justo in pellentesque iaculis. Nunc in elementum tortor. Vestibulum tincidunt lacus ac libero gravida, sit amet rhoncus risus iaculis. Sed rhoncus nisl ac felis

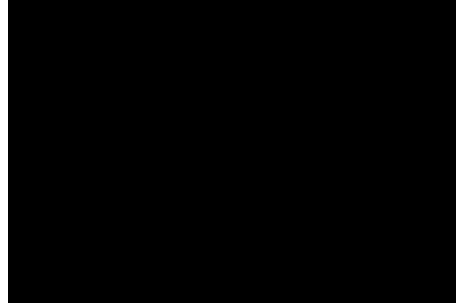


Figure 9.1: Lorem ipsum dolor sit amet, consectetur adipiscing elit. Ut et leo non tortor viverra sodales.

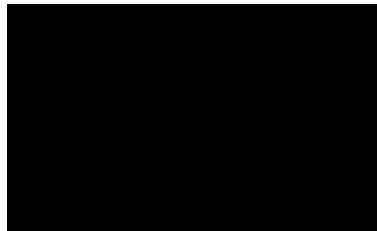


Figure 9.2: Ut condimentum odio orci, a varius sapien vehicula quis.

auctor efficitur. Nulla vel lorem bibendum, laoreet risus vel, euismod odio. Sed a justo augue. Sed sed viverra magna. Etiam vestibulum tellus ut consequat ultricies. Pellentesque mattis odio ac ipsum luctus, ac laoreet ex efficitur. Sed tincidunt, est id viverra ullamcorper, orci dolor accumsan erat, id accumsan tortor est quis ante. Integer pretium elit a ligula tristique imperdiet.

In vitae elit massa. Morbi fermentum arcu quis tristique pretium. Suspendisse potenti. Suspendisse at nisi nec sem dignissim mattis finibus ac sem. Aenean lobortis volutpat turpis, a lacinia ante pellentesque eget. Vivamus fermentum tempus viverra. Sed sollicitudin cursus rutrum. [25]

9.1.1 Fusce Convallis

Fusce convallis placerat porta. Nam porta euismod justo, nec efficitur erat tincidunt non. Proin viverra sagittis nibh, ac rhoncus nibh condimentum in. Nunc tristique augue quis ante

dapibus, sit amet porta purus molestie. Pellentesque sagittis tincidunt eros, eget fermentum nibh viverra dapibus. Phasellus id dignissim sapien. Mauris eget interdum sapien, in hendrerit ante.

Fusce sed eros sem. Mauris posuere egestas risus et sollicitudin. Suspendisse posuere nec lectus a iaculis. In tincidunt nisl consequat sem feugiat mollis. Vivamus ante libero, lobortis id erat vel, fringilla sodales justo. Mauris vel iaculis lectus, non vehicula ipsum. Praesent mollis convallis nibh in ornare. Fusce tincidunt libero sit amet efficitur convallis.

9.2 Curabitur

Curabitur dignissim orci quis orci blandit blandit.¹ Cras cursus tellus quam, sed lacinia nisi scelerisque posuere. Vestibulum sed lacinia orci, id sagittis lorem. Etiam lacinia elementum tortor, ut rutrum tellus laoreet sit amet. Etiam dignissim sagittis sapien in dignissim. Vestibulum ante ipsum primis in faucibus orci luctus et ultrices posuere cubilia Curae; Nullam blandit est vel diam hendrerit posuere. Maecenas nec arcu eu dui semper porttitor.

¹Aenean a semper dolor.

X	O	
O	X	
O		X

Table 9.1: Nulla suscipit ultricies massa at sagittis.

Suspendisse aliquet vel orci volutpat imperdiet. Aenean et ex a nisl volutpat ultrices. Duis pellentesque mi vitae maximus sagittis. Quisque dignissim ante pulvinar, porta odio sed, hendrerit ante. Mauris euismod enim ac nibh laoreet, vel eleifend lacus euismod. Fusce bibendum malesuada magna vitae efficitur.

APPENDICES

Appendix A

Etiam a Convallis

Your appendix goes here.

—

Lorem ipsum dolor sit amet, consectetur adipiscing elit. Sed cursus, ex vitae sagittis tempor, risus ipsum ultrices elit, vel eleifend magna ex in tellus. Proin congue mattis sem, eget gravida tellus iaculis nec. Sed consectetur varius quam convallis tincidunt. Aliquam congue augue vitae lacus dignissim, efficitur condimentum magna lacinia.

Etiam a convallis quam, in feugiat purus. Mauris porta magna ipsum, ac pharetra nisl tristique ac. Nullam consectetur finibus tortor, eget ultrices libero auctor a. Cras facilisis sapien metus, at accumsan ex auctor a. Pellentesque varius non dolor vitae rhoncus. Cras eget ante vitae magna aliquam condimentum. Vestibulum ante ipsum primis in faucibus orci luctus et ultrices posuere cubilia Curae; Donec molestie est consequat maximus dictum.[25]

Nunc Nec Ultrices Justo

Nunc nec ultrices justo, nec rhoncus urna. Proin sagittis tempor purus, nec pulvinar leo varius eget. Etiam a nisi nec neque dignissim molestie. Ut tincidunt vel diam sed imperdiet. Praesent a auctor turpis, in semper ipsum. Sed eu erat interdum, sagittis lectus nec, fringilla felis. Nunc lacus lacus, scelerisque eu mollis ac, ultrices a leo. Aliquam mattis felis enim, in cursus augue dignissim eget. Aenean fermentum mi id facilisis pulvinar.[25]

Aliquam aliquam, lorem elementum mollis ornare, augue felis tristique est, a blandit velit
dui a orci. Sed id nisl dictum, tincidunt dui quis, gravida felis. Curabitur vitae erat at lacus
volutpat iaculis ut ut enim. Nullam vel venenatis metus. Sed rutrum est at lectus elementum
viverra. Nulla sed enim risus.

Appendix B

Nulla Feugiat

1	2	3
4	5	6
7	8	9

Table B.1: Lorem ipsum dolor sit amet, consectetur adipiscing elit. Nulla feugiat ante quis consectetur pellentesque. In tincidunt orci in justo tempor, non tempor metus congue.[25]

Appendix C

Angular Momentum Coupling

Two angular momenta, $|j_1 m_1\rangle$ and $|j_2 m_2\rangle$, can be coupled into a state with total angular momentum J and projection M , $|j_1 j_2; JM\rangle$. The coupled state is written as a linear combination of uncoupled states, $|j_1 m_1; j_2 m_2\rangle$.

$$|j_1 j_2; JM\rangle = \sum_{m_1+m_2=M} \langle j_1 m_1; j_2 m_2 | JM \rangle |j_1 m_1; j_2 m_2\rangle \quad (\text{C.1})$$

The coefficients in this expansion, $\langle j_1 m_1; j_2 m_2 | JM \rangle$, are called the Clebsch-Gordon coefficients. They have the symmetry property that introduces a relative phase between states with different coupling orders.

$$\langle j_2 m_2; j_1 m_1 | JM \rangle = (-1)^{j_1+j_2-J} \langle j_1 m_1; j_2 m_2 | JM \rangle \quad (\text{C.2})$$

Appendix D

Coupled Two-Body State

A two-body state relative to some reference vacuum, $|\Phi\rangle$, involving either particles or holes, can be written as the result of acting with the appropriate particle or hole creation operators, $|pq\rangle = p^\dagger q^\dagger |\Phi\rangle$. The letters $\{p, q, r, s, \dots\}$ denote generic particle or hole states, $\{a, b, c, d, \dots\}$ denote particle states, and $\{i, j, k, l, \dots\}$ denote hole states. These M -scheme states, with total angular momentum projection M , can be used to build J -scheme states which are coupled to a total angular momentum J . The generic j -coupled states corresponding to the orbits of p and q are given by $\{\alpha, \beta, \gamma, \dots\}$.

$$|\alpha\beta; JM\rangle = \frac{\sqrt{1 + \delta_{\alpha\beta} (-1)^J}}{1 + \delta_{\alpha\beta}} \left[\alpha^\dagger \beta^\dagger \right]_{JM} |\Phi\rangle = \frac{\sqrt{1 + \delta_{\alpha\beta} (-1)^J}}{1 + \delta_{\alpha\beta}} \sum_{\substack{p \in \alpha \\ q \in \beta}} \langle j_p m_p j_q m_q | JM \rangle p^\dagger q^\dagger |\Phi\rangle \quad (\text{D.1})$$

When the states α and β are coupled in the reverse order, each Clebsch-Gordon coefficient acquires the same phase factor as Eqn. (2) when p and q are switched. Therefore the coupled states show a similar symmetry property as the Clebsch-Gordon coefficients depending on the order of α and β . An additional factor of (-1) comes from anti-commutating the creation operators involved, which must commute because they are only of the particle/hole creation type.

$$|\beta\alpha; JM\rangle = (-1)^{j_\alpha + j_\beta - J + 1} |\alpha\beta; JM\rangle \quad (\text{D.2})$$

Appendix E

Convergence Acceleration: Direct-Inversion of the Iterative Subspace

Direct-Inversion of the Iterative Subspace (DIIS) is an extension to the damping method to help stabilize and accelerate the convergence. In the damping method, the input amplitude vector to iteration $i + 1$ is a mixture of the output of the two previous iterations, $\tilde{\mathbf{t}}_{i+1} = \alpha \mathbf{t}_i + (1 - \alpha) \mathbf{t}_{i-1}$, where the CCD step is $\mathcal{F}(\tilde{\mathbf{t}}_i) = \mathbf{t}_i$. In DIIS, the input amplitude vector to iteration $i + 1$ is a linear combination of the last l vectors, $\tilde{\mathbf{t}}_{i+1} = \sum_{m=i-l+1}^i c_m \mathbf{t}_m$. Rewriting the vectors as the exact solution, $\mathcal{F}(\mathbf{t}^*) = \mathbf{t}^*$ or $\tilde{\mathbf{t}}_i = \mathbf{t}_i$, plus an error term, $\mathbf{t}_i = \mathbf{t}^* + \mathbf{r}_i$, the interpolated vector can be rewritten, $\tilde{\mathbf{t}}_{i+1} = \sum_{m=i-l+1}^i c_m (\mathbf{t}^* + \mathbf{r}_m) = \sum_{m=i-l+1}^i c_m \mathbf{t}^* + \sum_{m=i-l+1}^i c_m \mathbf{r}_m$. Equating this to the exact solution and minimizing the error vector gives, $\mathbf{t}^* = \lim \left(\sum_{m=i-l+1}^i c_m \mathbf{t}^* + \sum_{m=i-l+1}^i c_m \mathbf{r}_m \right) = \sum_{m=i-l+1}^i c_m \mathbf{t}^*$, so that $\sum_{m=i-l+1}^i c_m = 1$. Therefore, the task is to minimize the norm of the error vector, $\tilde{\mathbf{r}}_{i+1}^\dagger \tilde{\mathbf{r}}_{i+1} = \sum_{m,n=i-l+1}^i c_m c_n \mathbf{r}_m^\dagger \mathbf{r}_n$, with the constraint that the sum of the coefficients is one, $\min \left(\sum_{m,n=i-l+1}^i c_m c_n \mathbf{r}_m^\dagger \mathbf{r}_n - \lambda \left(1 - \sum_{m=i-l+1}^i c_m \right) \right)$. This can be rewritten as a matrix equation with matrix $B_{ij} = \mathbf{r}_i^\dagger \mathbf{r}_j$, $\mathcal{L} = \sum_{m,n=i-l+1}^i c_m c_n B_{mn} - \lambda \left(1 - \sum_{m=i-l+1}^i c_m \right)$.

$$\frac{\partial \mathcal{L}}{\partial c_k} = 0 = \sum_{n=i-l+1}^i c_n B_{kn} + \sum_{m=i-l+1}^i c_m B_{mk} + \lambda = 2 \sum_{n=i-l+1}^i c_n B_{kn} + \lambda \quad (\text{E.1})$$

$$(\text{E.2})$$

Appendix F

CCSD Diagrams

The following diagrams represent the different contributions to the CCSD cluster amplitudes *without* directly building the effective Hamiltonian, \bar{H} . The boxed diagrams are automatically zero in a Hartree-Fock basis.

$$\begin{aligned}
 \hat{f}_N \hat{t}_1 |\Phi_0\rangle_c &= \boxed{\text{diagram 1}} + \text{diagram 2} + \text{diagram 3} \\
 &= \boxed{f_i^a} - \sum_k f_i^k t_k^a + \sum_c f_c^a t_i^c
 \end{aligned} \tag{F.1}$$

The diagrams in equation (F.1) are as follows:
 - **Diagram 1 (boxed):** A vertex with two incoming lines labeled a and i , and a dashed line extending to the right ending in a cross. This diagram is enclosed in a dashed box.
 - **Diagram 2:** A vertex with two incoming lines labeled a and i , and two outgoing lines labeled k and c . The vertex is connected to a horizontal bar below it. A dashed line extends to the right ending in a cross.
 - **Diagram 3:** A vertex with two incoming lines labeled i and a , and two outgoing lines labeled c and k . The vertex is connected to a horizontal bar below it. A dashed line extends to the right ending in a cross.

$$\begin{aligned}
 \hat{V}_N \hat{t}_1 |\Phi_0\rangle_c &= \text{diagram 4} \\
 &= - \sum_{kc} V_{ic}^{ka} t_k^c
 \end{aligned} \tag{F.2}$$

The diagram in equation (F.2) is as follows:
 - **Diagram 4:** A vertex with two incoming lines labeled a and i , and two outgoing lines labeled c and k . The vertex is connected to a horizontal bar below it. A dashed line extends to the right ending in a cross.

$$\begin{aligned}
\hat{f}_N \hat{t}_2 |\Phi_0\rangle_c &= \text{Diagram: A vertex with an incoming line from the left labeled 'c' and an outgoing line to the right labeled 'i'. A loop is attached to the vertex, with a horizontal line below it. A dashed line with an 'X' at its end extends from the vertex to the left. The entire diagram is enclosed in a dashed box.} \\
&= \sum_{kc} f_c^k t_{ki}^{ac}
\end{aligned} \tag{F.3}$$

$$\begin{aligned}
\hat{V}_N \hat{t}_2 |\Phi_0\rangle_c &= \text{Diagram 1: A vertex with an incoming line from the left labeled 'c' and an outgoing line to the right labeled 'i'. A loop is attached to the vertex, with a horizontal line below it. A dashed line with an 'X' at its end extends from the vertex to the left.} + \text{Diagram 2: A vertex with an incoming line from the left labeled 'c' and an outgoing line to the right labeled 'a'. A loop is attached to the vertex, with a horizontal line below it. A dashed line with an 'X' at its end extends from the vertex to the left.} \\
&= \frac{1}{2} \sum_{kcd} V_{cd}^{ka} t_{ki}^{cd} + \frac{1}{2} \sum_{klc} V_{ic}^{kl} t_{kl}^{ca}
\end{aligned} \tag{F.4}$$

$$\begin{aligned}
\hat{f}_N \hat{t}_1^2 |\Phi_0\rangle_c &= \text{Diagram: Two vertices connected by a horizontal line. The left vertex has an incoming line from the left labeled 'a' and an outgoing line to the right labeled 'l'. The right vertex has an incoming line from the left labeled 'd' and an outgoing line to the right labeled 'i'. A dashed line with an 'X' at its end extends from the right vertex to the right. The entire diagram is enclosed in a dashed box.} \\
&= \sum_{kcd} f_d^l t_l^a t_i^d
\end{aligned} \tag{F.5}$$

$$\begin{aligned}
\hat{V}_N \hat{t}_1^2 |\Phi_0\rangle_c &= \text{diagram 1} + \text{diagram 2} \\
&= \sum_{kcd} V_{cd}^{ka} t_k^c t_i^d + \sum_{klc} V_{ic}^{kl} t_k^c t_l^a
\end{aligned} \tag{F.6}$$

The diagrams show two vertices connected by a dashed line. In the first diagram, the left vertex has incoming lines \$c\$ and \$k\$ and an outgoing loop \$c \to k\$. The right vertex has incoming lines \$d\$ and \$i\$ and an outgoing line \$a\$. In the second diagram, the left vertex has an incoming line \$c\$ and an outgoing loop \$c \to k\$. The right vertex has incoming lines \$l\$ and \$i\$ and an outgoing line \$a\$.

$$\begin{aligned}
\hat{V}_N \hat{t}_1 \hat{t}_2 |\Phi_0\rangle_c &= \text{diagram 1} + \text{diagram 2} + \text{diagram 3} \\
&= -\frac{1}{2} \sum_{klcd} V_{cd}^{kl} t_{ki}^{cd} t_l^a - \frac{1}{2} \sum_{klcd} V_{cd}^{kl} t_{kl}^{ca} t_i^d + \sum_{klcd} V_{cd}^{kl} t_{il}^{ad} t_k^c
\end{aligned} \tag{F.7}$$

The diagrams show three vertices. Diagram 1: Left vertex has incoming \$a\$ and outgoing \$l\$; middle vertex has incoming \$d\$ and outgoing \$i\$; right vertex has an outgoing loop \$c \to k\$. Diagram 2: Left vertex has incoming \$i\$ and outgoing \$d\$; middle vertex has incoming \$l\$ and outgoing \$a\$; right vertex has an outgoing loop \$c \to k\$. Diagram 3: Left vertex has an outgoing loop \$c \to k\$; middle vertex has an outgoing loop \$d \to l\$; right vertex has incoming \$a\$ and outgoing \$i\$.

$$\begin{aligned}
\hat{V}_N \hat{t}_1^3 |\Phi_0\rangle_c &= \text{diagram} \\
&= - \sum_{klcd} V_{cd}^{kl} t_k^c t_i^d t_l^a
\end{aligned} \tag{F.8}$$

The diagram shows three vertices. The left vertex has incoming \$a\$ and outgoing \$l\$; the middle vertex has incoming \$d\$ and outgoing \$i\$; the right vertex has an outgoing loop \$c \to k\$.

$$\begin{aligned}
\hat{V}_N |\Phi_0\rangle_c &= \text{diagram} \\
&= V_{ij}^{ab}
\end{aligned} \tag{F.9}$$

The diagram shows two vertices connected by a dashed line. The left vertex has incoming lines \$a\$ and \$i\$, and the right vertex has incoming lines \$b\$ and \$j\$.

$$\begin{aligned}
\hat{f}_N \hat{t}_2 |\Phi_0\rangle_c &= \text{Diagram 1} + \text{Diagram 2} \\
&= \hat{P}(ab) \sum_c f_c^b t_{ij}^{ac} - \hat{P}(ij) \sum_k f_j^k t_{ik}^{ab}
\end{aligned} \tag{F.10}$$

Diagram 1: A vertex with four external lines. Two lines (labeled i and a) enter from the left, and two lines (labeled j and c) exit to the right. A dashed line connects the two internal vertices, with a cross at its right end.

Diagram 2: A vertex with four external lines. Two lines (labeled a and i) enter from the left, and two lines (labeled b and j) exit to the right. A dashed line connects the two internal vertices, with a cross at its right end.

$$\begin{aligned}
\hat{V}_N \hat{t}_1 |\Phi_0\rangle_c &= \text{Diagram 3} + \text{Diagram 4} \\
&= -\hat{P}(ab) \sum_k V_{ij}^{kb} t_k^a + \hat{P}(ij) \sum_c V_{cj}^{ab} t_i^c
\end{aligned} \tag{F.11}$$

Diagram 3: A vertex with four external lines. Two lines (labeled a and k) enter from the left, and two lines (labeled i and j) exit to the right. A dashed line connects the two internal vertices.

Diagram 4: A vertex with four external lines. Two lines (labeled i and c) enter from the left, and two lines (labeled a and b) exit to the right. A dashed line connects the two internal vertices.

$$\begin{aligned}
\hat{V}_N \hat{t}_2 |\Phi_0\rangle_c &= \text{Diagram 5} + \text{Diagram 6} + \text{Diagram 7} \\
&= \frac{1}{2} \sum_{kl} V_{ij}^{kl} t_{kl}^{ab} + \frac{1}{2} \sum_{cd} V_{cd}^{ab} t_{ij}^{cd} - \hat{P}(ij|ab) \sum_{kc} V_{ic}^{kb} t_{kj}^{ac}
\end{aligned} \tag{F.12}$$

Diagram 5: A vertex with four external lines. Two lines (labeled a and k) enter from the left, and two lines (labeled i and j) exit to the right. A dashed line connects the two internal vertices.

Diagram 6: A vertex with four external lines. Two lines (labeled i and c) enter from the left, and two lines (labeled a and b) exit to the right. A dashed line connects the two internal vertices.

Diagram 7: A vertex with four external lines. Two lines (labeled a and k) enter from the left, and two lines (labeled i and j) exit to the right. A dashed line connects the two internal vertices.

$$\begin{aligned}
\hat{V}_N \hat{t}_1^2 |\Phi_0\rangle_c &= \text{Diagram 8} + \text{Diagram 9} + \text{Diagram 10} \\
&= \sum_{kl} V_{ij}^{kl} t_k^a t_l^b + \sum_{cd} V_{cd}^{ab} t_i^c t_j^d - \hat{P}(ij|ab) \sum_{kc} V_{ic}^{kb} t_k^a t_j^c
\end{aligned} \tag{F.13}$$

Diagram 8: Two vertices connected by a dashed line. The left vertex has external lines a, k, i, j and the right vertex has external lines b, l, i, j .

Diagram 9: Two vertices connected by a dashed line. The left vertex has external lines i, c, a, b and the right vertex has external lines j, d, a, b .

Diagram 10: Two vertices connected by a dashed line. The left vertex has external lines a, k, i, j and the right vertex has external lines b, c, i, j .

$$\begin{aligned}
\hat{V}_N \hat{t}_2^2 |\Phi_0\rangle_c &= \text{Diagram 1} + \text{Diagram 2} + \text{Diagram 3} \\
&+ \text{Diagram 4} \\
&= \frac{1}{4} \sum_{klcd} V_{cd}^{kl} t_{kl}^{ab} t_{ij}^{cd} + \hat{P}(ab) \sum_{klcd} V_{cd}^{kl} t_{lj}^{ac} t_{ki}^{bd} - \hat{P}(ij) \frac{1}{2} \sum_{klcd} V_{cd}^{kl} t_{lj}^{ab} t_{ki}^{cd} \\
&- \hat{P}(ab) \frac{1}{2} \sum_{klcd} V_{cd}^{kl} t_{ij}^{db} t_{kl}^{ca} \tag{F.14}
\end{aligned}$$

$$\begin{aligned}
\hat{f}_N \hat{t}_1 \hat{t}_2 |\Phi_0\rangle_c &= \text{Diagram 5} + \text{Diagram 6} \\
&= - \left[\hat{P}(ab) \sum_{kc} f_c^k t_k^a t_{ij}^{cb} \right] - \left[\hat{P}(ij) \sum_{kc} f_c^k t_i^c t_{kj}^{ab} \right] \tag{F.15}
\end{aligned}$$

$$\begin{aligned}
\hat{V}_N \hat{t}_1 \hat{t}_2 |\Phi_0\rangle_c &= \text{Diagram 1} + \text{Diagram 2} + \text{Diagram 3} \\
&+ \text{Diagram 4} + \text{Diagram 5} + \text{Diagram 6} \\
&= \hat{P}(ij|ab) \sum_{kcd} V_{cd}^{ka} t_{jk}^{bc} t_i^d - \hat{P}(ij|ab) \sum_{klc} V_{ci}^{kl} t_{jk}^{bc} t_l^a - \hat{P}(ab) \frac{1}{2} \sum_{kcd} V_{cd}^{kb} t_{ij}^{cd} t_k^a \\
&+ \hat{P}(ij) \frac{1}{2} \sum_{klc} V_{cj}^{kl} t_{kl}^{ab} t_i^c + \hat{P}(ab) \sum_{kcd} V_{cd}^{ka} t_k^c t_{ij}^{db} - \hat{P}(ij) \sum_{klc} V_{ci}^{kl} t_k^c t_{lj}^{ab} \quad (\text{F.16})
\end{aligned}$$

$$\begin{aligned}
\hat{V}_N \hat{t}_1^3 |\Phi_0\rangle_c &= \text{Diagram 7} + \text{Diagram 8} \\
&= -\hat{P}(ij|ab) \sum_{kcd} V_{cd}^{kb} t_k^a t_i^c t_j^d + \hat{P}(ij|ab) \sum_{klc} V_{cj}^{kl} t_i^c t_k^a t_l^b \quad (\text{F.17})
\end{aligned}$$

$$\begin{aligned}
\hat{V}_N \hat{t}_1^2 \hat{t}_2 |\Phi_0\rangle_c &= \text{Diagram 1} + \text{Diagram 2} + \text{Diagram 3} \\
&+ \text{Diagram 4} + \text{Diagram 5} \\
&= \frac{1}{2} \sum_{klcd} V_{cd}^{kl} t_{kl}^{ab} t_i^c t_j^d + \frac{1}{2} \sum_{klcd} V_{cd}^{kl} t_{ij}^{cd} t_k^a t_l^b + \hat{P}(ij|ab) \sum_{klcd} V_{cd}^{kl} t_{lj}^{ac} t_k^b t_i^d \\
&- \hat{P}(ij) \frac{1}{2} \sum_{klcd} V_{cd}^{kl} t_{lj}^{ab} t_k^c t_i^d - \hat{P}(ab) \frac{1}{2} \sum_{klcd} V_{cd}^{kl} t_{ij}^{db} t_k^c t_l^a
\end{aligned} \tag{F.18}$$

$$\begin{aligned}
\hat{V}_N \hat{t}_1^4 |\Phi_0\rangle_c &= \text{Diagram 6} \\
&= \sum_{klcd} V_{cd}^{kl} t_k^a t_l^b t_i^c t_j^d
\end{aligned} \tag{F.19}$$

Appendix G

Computational Implementation

The sums involved in building the CC effective Hamiltonian, solving the CC equations, solving the EOM-CC equations, and building effective operators can all be reformulated as matrix-matrix multiplications and thus performed with efficient LAPACK and BLAS routines. To take advantage of this efficiency, the various cluster amplitudes and matrix elements must be grouped into structures with similar index structure. An additional benefit to these structures is that angular-momentum-coupling coefficients are automatically removed by summing over Clebsch-Gordon coefficients ($\sum_{m_1 m_2} C_{m_1 m_2 M}^{j_1 j_2 J} C_{m_1 m_2 M'}^{j_1 j_2 J'} = \delta_{JJ'} \delta_{MM'}$).

Structure Definitions

The matrix structures are based on channels that separate states with different symmetries depending on a system's conserved quantum numbers, given by $\vec{\xi}$, so that $|p\rangle \in \vec{\xi}_3$. This separation can be applied to direct two-body states ($|pq\rangle \rightarrow \vec{\xi}_p + \vec{\xi}_q \in \vec{\xi}_1$) and cross two-body states ($|p\bar{q}\rangle \rightarrow \vec{\xi}_p - \vec{\xi}_q \in \vec{\xi}_2$). Additionally, cross three-body states can be separated as one-body states ($|pq\bar{s}\rangle \rightarrow \vec{\xi}_p + \vec{\xi}_q - \vec{\xi}_r \in \vec{\xi}_3$).

For a one-body operator $A_q^p \left\{ \hat{p}^\dagger \hat{q} \right\}$, there is a direct-channel matrix element and a cross-channel matrix element,

$$\mathbf{A}_1 = A_q^p \quad \mathbf{A}_2 = A^{p\bar{q}} \quad (\text{G.1})$$

For a two-body operator $A_{rs}^{pq} \left\{ \hat{p}^\dagger \hat{q}^\dagger \hat{s} \hat{r} \right\}$, there is a direct-channel matrix element, four

cross-channel matrix elements, and four one-channel matrix elements,

$$\begin{aligned}
\mathbf{A}_1 &= A_{rs}^{pq} \\
\mathbf{A}_{2_1} &= A_{r\bar{q}}^{p\bar{s}} \quad \mathbf{A}_{2_2} = A_{s\bar{p}}^{q\bar{r}} \quad \mathbf{A}_{2_3} = A_{s\bar{q}}^{p\bar{r}} \quad \mathbf{A}_{2_4} = A_{r\bar{p}}^{q\bar{s}} \\
\mathbf{A}_{3_1} &= A_{rs\bar{q}}^p \quad \mathbf{A}_{3_2} = A_{rs\bar{p}}^q \quad \mathbf{A}_{3_3} = A_r^{pq\bar{s}} \quad \mathbf{A}_{3_4} = A_s^{pq\bar{r}}
\end{aligned} \tag{G.2}$$

For an EOM operator of the form $A_r^{pq} \left\{ \hat{p}^\dagger \hat{q}^\dagger \hat{r} \right\}$, there is a direct-channel matrix element, a one-channel matrix element, and two cross-channel matrix elements,

$$\begin{aligned}
\mathbf{A}_1 &= A_r^{pq} & \mathbf{A}_3 &= A^{pq\bar{r}} \\
\mathbf{A}_{2_1} &= A_{r\bar{q}}^p & \mathbf{A}_{2_2} &= A_{r\bar{p}}^q
\end{aligned} \tag{G.3}$$

EOM operators of the form $A_{qr}^p \left\{ \hat{p}^\dagger \hat{r} \hat{q} \right\}$ has similar structures,

$$\begin{aligned}
\mathbf{A}_1 &= A_{qr}^p & \mathbf{A}_3 &= A_{qr\bar{p}} \\
\mathbf{A}_{2_1} &= A_q^{p\bar{r}} & \mathbf{A}_{2_2} &= A_r^{p\bar{q}}
\end{aligned} \tag{G.4}$$

\bar{H} , Matrix Form

$$\begin{aligned}
X_a^i &= \boxed{f_a^i} + V_{ck}^{i\bar{a}} t^{c\bar{k}} \\
X_2^{hp} &\leftarrow \boxed{f_2^{hp}} + V_{23}^{hhpp} \cdot t_2
\end{aligned} \tag{G.5}$$

$$\begin{aligned}
X_b^a &= f_b^a - \frac{1}{2} t_{kl\bar{c}}^a V_b^{kl\bar{c}} + V_{c\bar{k}}^{a\bar{l}} t^{c\bar{k}} - t_k^a X_b^k \\
X_3^{pp} &\longleftarrow -\frac{1}{2} t_{31} \cdot V_{33}^{hhpp} - t_3 \cdot X_3^{hp} \\
X_2^{pp} &\longleftarrow f_2^{pp} + V_{24}^{hppp} \cdot t_2
\end{aligned} \tag{G.6}$$

$$\begin{aligned}
X_j^i &= f_j^i + \frac{1}{2} V_{cd\bar{k}}^i t_j^{cd\bar{k}} + V_{c\bar{k}}^{i\bar{j}} t^{c\bar{k}} \\
X_3^{thh} &\longleftarrow \frac{1}{2} V_{31}^{hhpp} \cdot t_{33} \\
X_2^{thh} &\longleftarrow f_2^{hh} + V_{23}^{hhhp} \cdot t_2
\end{aligned} \tag{G.7}$$

$$\begin{aligned}
X_j^i &= f_j^i + \frac{1}{2} V_{cd\bar{k}}^i t_j^{cd\bar{k}} + V_{c\bar{k}}^{i\bar{j}} t^{c\bar{k}} + X_c^i t_j^c \\
X_3^{hh} &\longleftarrow \frac{1}{2} V_{31}^{hhpp} \cdot t_{33} + X_3^{hp} \cdot t_3 \\
X_2^{thh} &\longleftarrow f_2^{hh} + V_{23}^{hhhp} \cdot t_2
\end{aligned} \tag{G.8}$$

$$\begin{aligned}
X_i^a &= \boxed{f_i^a} + X_c^a t_i^c - t_k^a X_i^k - V_{c\bar{k}}^{a\bar{l}} t^{c\bar{k}} + \frac{1}{2} V_{cd\bar{k}}^a t_i^{cd\bar{k}} - \frac{1}{2} t_{kl\bar{c}}^a V_i^{kl\bar{c}} + t_{k\bar{c}}^{a\bar{l}} X^{k\bar{c}} \\
X_3^{ph} &\longleftarrow X_3^{pp} \cdot t_3 - t_3 \cdot X_3^{thh} + \frac{1}{2} V_{32}^{hppp} \cdot t_{34} - \frac{1}{2} t_{31} \cdot V_{33}^{hhhp} \\
X_2^{ph} &\longleftarrow \boxed{f_2^{ph}} - V_{22}^{hphp} \cdot t_2 + t_{23} \cdot X_2^{hp}
\end{aligned} \tag{G.9}$$

$$\begin{aligned}
X_{bc}^{ia} &= V_{bc}^{ia} - \frac{1}{2} t_k^a V_{bc\bar{i}}^k \\
X_{32}^{hppp} &\longleftarrow V_{32}^{hppp} - \frac{1}{2} t_3 \cdot V_{32}^{hhpp}
\end{aligned} \tag{G.10}$$

$$\begin{aligned}
X_{bc}^{ia} &= V_{bc}^{ia} - t_k^a V_{bc\bar{i}}^k \\
X_{32}^{hppp} &\longleftarrow V_{32}^{hppp} - t_3 \cdot V_{32}^{hhpp}
\end{aligned} \tag{G.11}$$

$$\begin{aligned}
X_{ka}^{ij} &= V_{ka}^{ij} + \frac{1}{2} V_c^{ij\bar{a}} t_k^c \\
X_{33}^{hhhp} &\longleftarrow V_{ka}^{ij} + \frac{1}{2} V_{33}^{hhpp} \cdot t_3
\end{aligned} \tag{G.12}$$

$$\begin{aligned}
X_{ka}^{ij} &= V_{ka}^{ij} + V_c^{ij\bar{a}} t_k^c \\
X_{33}^{hhhp} &\longleftarrow V_{ka}^{ij} + V_{33}^{hhpp} \cdot t_3
\end{aligned} \tag{G.13}$$

$$\begin{aligned}
X_{cd}'^{ab} &= V_{cd}^{ab} - \hat{P}(ab) t_k^a X_{cd\bar{b}}'^k \\
X_1'^{pppp} &\longleftarrow V_1^{pppp} \\
X_{31}'^{pppp} &\longleftarrow -t_3 \cdot X_{31}^{hppp} \\
X_{32}'^{pppp} &\longleftarrow t_3 \cdot X_{31}^{hppp}
\end{aligned} \tag{G.14}$$

$$\begin{aligned}
X_{cd}^{ab} &= X_{cd}'^{ab} + \frac{1}{2} t_{kl}^{ab} V_{cd}^{kl} \\
X_1^{pppp} &\longleftarrow X_1'^{pppp} + \frac{1}{2} t_1 \cdot V_1^{hhpp}
\end{aligned} \tag{G.15}$$

$$\begin{aligned}
X_{kl}^{ij} &= V_{kl}^{ij} + \frac{1}{2} V_{cd}^{ij} t_{kl}^{cd} + \hat{P}(kl) X_c^{ij\bar{k}} t_l^c \\
X_1^{hhhh} &\longleftarrow V_1^{hhhh} + \frac{1}{2} V_1^{hhpp} \cdot t_1 \\
X_{34}^{hhhh} &\longleftarrow X_{34}^{hhhp} \cdot t_3 \\
X_{33}^{hhhh} &\longleftarrow -X_{34}^{hhhp} \cdot t_3
\end{aligned} \tag{G.16}$$

$$\begin{aligned}
X_{jb}^{ia} &= V_{jb}^{ia} + X_c^{ia\bar{b}} t_j^c - \frac{1}{2} t_k^a V_{jb\bar{i}}^k \\
X_{21}^{hphp} &\longleftarrow V_{21}^{hphp} \\
X_{33}^{hphp} &\longleftarrow X_{33}^{hppp} \cdot t_3 \\
X_{32}^{hphp} &\longleftarrow -\frac{1}{2} t_3 \cdot V_{32}^{hhhp}
\end{aligned} \tag{G.17}$$

$$\begin{aligned}
X_{jb}^{ia} &= V_{jb}^{ia} + \frac{1}{2} X_c^{ia\bar{b}} t_j^c - \frac{1}{2} t_k^a V_{jb\bar{i}}^k \\
X_{21}^{hhph} &\longleftarrow V_{21}^{hhph} \\
X_{33}^{hhph} &\longleftarrow \frac{1}{2} X_{33}^{hppp} \cdot t_3 \\
X_{32}^{hhph} &\longleftarrow -\frac{1}{2} t_3 \cdot V_{32}^{hhhp}
\end{aligned} \tag{G.18}$$

$$\begin{aligned}
X_{jb}^{ia} &= V_{jb}^{ia} + \frac{1}{2} X_c^{ia\bar{b}} t_j^c - t_k^a V_{jb\bar{i}}^k \\
X_{21}^{hhph} &\longleftarrow V_{21}^{hhph} \\
X_{33}^{hhph} &\longleftarrow \frac{1}{2} X_{33}^{hppp} \cdot t_3 \\
X_{32}^{hhph} &\longleftarrow -t_3 \cdot V_{32}^{hhhp}
\end{aligned} \tag{G.19}$$

$$\begin{aligned}
X_{jb}^{ia} &= V_{jb}^{ia} + X_c^{iab} t_j^c - t_k^a V_{jb\bar{i}}^k - \left(\frac{1}{2}\right) V_{c\bar{k}}^{i\bar{b}} t_{j\bar{a}}^{c\bar{k}} \\
X_{21}^{hphp} &\longleftarrow V_{21}^{hphp} - \left(\frac{1}{2}\right) V_{21}^{hphp} t_{21} \\
X_{33}^{hphp} &\longleftarrow X_{33}^{hphp} \cdot t_3 \\
X_{32}^{hphp} &\longleftarrow -t_3 \cdot V_{32}^{hhhp}
\end{aligned} \tag{G.20}$$

$$\begin{aligned}
X_{ic}'^{ab} &= V_{ic}^{ab} + \frac{1}{2} V_d^{ab\bar{c}} t_i^d - \hat{P}(ab) t_k^a X_{ic\bar{b}}''^k \\
X_{33}'^{pphp} &\longleftarrow V_{33}^{pphp} + \frac{1}{2} V_{33}^{pppp} \cdot t_3 \\
X_{31}'^{pphp} &\longleftarrow -t_3 \cdot X_{31}''^{hphp} \\
X_{32}'^{pphp} &\longleftarrow t_3 \cdot X_{31}'''^{hphp}
\end{aligned} \tag{G.21}$$

$$\begin{aligned}
X_{ic}^{ab} &= V_{ic}^{ab} + V_d^{ab\bar{c}} t_i^d - \hat{P}(ab) t_k^a X_{ic\bar{b}}'^k - t_k^{ab\bar{i}} X_c^k + \hat{P}(ab) t_{k\bar{d}}^{a\bar{i}} X_{c\bar{b}}^{k\bar{d}} + \frac{1}{2} t_{kl}^{ab} X_{ic}^{kl} \\
X_{33}^{pphp} &\longleftarrow V_{33}^{pphp} + V_{33}^{pppp} \cdot t_3 \\
X_{31}^{pphp} &\longleftarrow -t_3 \cdot X_{31}'^{hphp} \\
X_{32}^{pphp} &\longleftarrow t_3 \cdot X_{31}''^{hphp} \\
X_{34}^{pphp} &\longleftarrow -t_{34} \cdot X_3^{hp} \\
X_{23}^{pphp} &\longleftarrow t_{23} \cdot X_{23}^{hphp} \\
X_{22}^{pphp} &\longleftarrow -t_{23} \cdot X_{23}^{hphp} \\
X_1^{pphp} &\longleftarrow \frac{1}{2} t_1 \cdot X_1^{hhhp}
\end{aligned} \tag{G.22}$$

$$\begin{aligned}
X_{jk}^{ia} &= V_{jk}^{ia} - \frac{1}{2} t_l^a V_{jk\bar{i}}^l \\
X_{32}^{hphh} &\longleftarrow V_{32}^{hphh} - \frac{1}{2} t_3 \cdot V_{32}^{hhhh}
\end{aligned} \tag{G.23}$$

$$\begin{aligned}
X_{jk}^{ia} &= V_{jk}^{ia} - t_l^a V_{jk\bar{i}}^l + \hat{P}(jk) X_c^{''ia\bar{j}} t_k^c + \hat{P}(jk) X_{c\bar{l}}^{i\bar{j}} t_{k\bar{a}}^{c\bar{l}} + \frac{1}{2} X_{cd}^{ia} t_{jk}^{cd} + X_c^{i\bar{j}} t_{jk\bar{a}}^c \\
X_{32}^{hphh} &\longleftarrow V_{32}^{hphh} - t_3 \cdot V_{32}^{hhhh} \\
X_{34}^{hphh} &\longleftarrow X_{34}^{''hphp} \cdot t_3 \\
X_{33}^{hphh} &\longleftarrow -X_{34}^{''hphp} \cdot t_3 \\
X_{23}^{hphh} &\longleftarrow X_{23}^{hhhp} \cdot t_{23} \\
X_{21}^{hphh} &\longleftarrow -X_{23}^{hhhp} \cdot t_{23} \\
X_1^{hphh} &\longleftarrow \frac{1}{2} X_1^{hppp} \cdot t_1 \\
X_{31}^{hphh} &\longleftarrow X_3^{hp} \cdot t_{31}
\end{aligned} \tag{G.24}$$

$$\begin{aligned}
X_{ij}^{ab} &= V_{ij}^{ab} + \hat{P}(ab) X_c^a t_{ij\bar{b}}^c - \hat{P}(ij) t_k^{ab\bar{j}} X_i^k + \frac{1}{2} X_{cd}'^{ab} t_{ij}^{cd} + \frac{1}{2} t_{kl}^{ab} X_{ij}^{kl} - \hat{P}(ab|ij) t_{k\bar{c}}^{a\bar{j}} X_{i\bar{b}}^{k\bar{c}} - \hat{P}(ab) t_k^a X_{ij\bar{b}}'^k + \hat{P} \\
X_1^{pphh} &\longleftarrow V_1^{pphh} + \frac{1}{2} X_1'^{pppp} \cdot t_1 + \frac{1}{2} t_1 \cdot X_1^{hhhh} \\
X_{3_1}^{pphh} &\longleftarrow X_3^{pp} \cdot t_{3_1} - t_3 X_{3_1}'^{hphh} \\
X_{3_2}^{pphh} &\longleftarrow -X_3^{pp} \cdot t_{3_1} + t_3 X_{3_1}'^{hphh} \\
X_{3_3}^{pphh} &\longleftarrow -t_{3_3} \cdot X_3^{hh} + X_{3_4}'^{pphp} t_3 \\
X_{3_4}^{pphh} &\longleftarrow t_{3_3} \cdot X_3^{hh} - X_{3_4}'^{pphp} t_3 \\
X_{2_1}^{pphh} &\longleftarrow -t_{2_1} \cdot X_{2_1}^{hphp} \\
X_{2_2}^{pphh} &\longleftarrow -t_{2_1} \cdot X_{2_1}^{hphp} \\
X_{2_3}^{pphh} &\longleftarrow t_{2_1} \cdot X_{2_1}^{hphp} \\
X_{2_4}^{pphh} &\longleftarrow t_{2_1} \cdot X_{2_1}^{hphp}
\end{aligned} \tag{G.25}$$

REFERENCES

REFERENCES

- [1] Derivation of the brueckner many-body theory. *Proceedings of the Royal Society of London A: Mathematical, Physical and Engineering Sciences*, 239(1217):267–279, 1957.
- [2] Frank T. Avignone, Steven R. Elliott, and Jonathan Engel. Double beta decay, majorana neutrinos, and neutrino mass. *Rev. Mod. Phys.*, 80:481–516, Apr 2008.
- [3] R. F. Bacher. The interaction of configurations: $sd - p^2$. *Phys. Rev.*, 43:264–269, Feb 1933.
- [4] F.C. Barker, B.A. Brown, W. Jaus, and G. Rasche. Determination of ν ud— from fermi decays and the unitarity of the km-mixing matrix. *Nuclear Physics A*, 540(3):501 – 519, 1992.
- [5] Bruce R. Barrett, Petr Navrátil, and James P. Vary. Ab initio no core shell model. *Progress in Particle and Nuclear Physics*, 69(Supplement C):131 – 181, 2013.
- [6] Rodney J. Bartlett and Monika Musiał. Coupled-cluster theory in quantum chemistry. *Rev. Mod. Phys.*, 79:291–352, Feb 2007.
- [7] Omar Benhar, Nicola Farina, Hiroki Nakamura, Makoto Sakuda, and Ryoichi Seki. Electron- and neutrino-nucleus scattering in the impulse approximation regime. *Phys. Rev. D*, 72:053005, Sep 2005.
- [8] H. A. Bethe. Nuclear many-body problem. *Phys. Rev.*, 103:1353–1390, Sep 1956.
- [9] Sven Binder, Piotr Piecuch, Angelo Calci, Joachim Langhammer, Petr Navrátil, and Robert Roth. Extension of coupled-cluster theory with a noniterative treatment of connected triply excited clusters to three-body hamiltonians. *Phys. Rev. C*, 88:054319, Nov 2013.
- [10] R. M. Bionta, G. Blewitt, C. B. Bratton, D. Casper, A. Ciocio, R. Claus, B. Cortez, M. Crouch, S. T. Dye, S. Errede, G. W. Foster, W. Gajewski, K. S. Ganezer, M. Goldhaber, T. J. Haines, T. W. Jones, D. Kielczewska, W. R. Kropp, J. G. Learned, J. M. LoSecco, J. Matthews, R. Miller, M. S. Mudan, H. S. Park, L. R. Price, F. Reines, J. Schultz, S. Seidel, E. Shumard, D. Sinclair, H. W. Sobel, J. L. Stone, L. R. Sulak, R. Svoboda, G. Thornton, J. C. van der Velde, and C. Wuest. Observation of a neutrino burst in coincidence with supernova 1987a in the large magellanic cloud. *Phys. Rev. Lett.*, 58:1494–1496, Apr 1987.
- [11] S. K. Bogner, H. Hergert, J. D. Holt, A. Schwenk, S. Binder, A. Calci, J. Langhammer, and R. Roth. Nonperturbative shell-model interactions from the in-medium similarity renormalization group. *Phys. Rev. Lett.*, 113:142501, Oct 2014.
- [12] S.K. Bogner, R.J. Furnstahl, and A. Schwenk. From low-momentum interactions to nuclear structure. *Progress in Particle and Nuclear Physics*, 65(1):94 – 147, 2010.

- [13] Charles G Broyden. A class of methods for solving nonlinear simultaneous equations. *Math. Comput.*, 19(92):577–593, 1965.
- [14] K. A. Brueckner and C. A. Levinson. Approximate reduction of the many-body problem for strongly interacting particles to a problem of self-consistent fields. *Phys. Rev.*, 97:1344–1352, Mar 1955.
- [15] S. Bustabad, G. Bollen, M. Brodeur, D. L. Lincoln, S. J. Novario, M. Redshaw, R. Ringle, S. Schwarz, and A. A. Valverde. First direct determination of the ^{48}Ca double- β decay q value. *Phys. Rev. C*, 88:022501, Aug 2013.
- [16] Nicola Cabibbo. Unitary symmetry and leptonic decays. *Phys. Rev. Lett.*, 10:531–533, Jun 1963.
- [17] J. Carlson, S. Gandolfi, F. Pederiva, Steven C. Pieper, R. Schiavilla, K. E. Schmidt, and R. B. Wiringa. Quantum monte carlo methods for nuclear physics. *Rev. Mod. Phys.*, 87:1067–1118, Sep 2015.
- [18] J. Cizek and J. Paldus. Correlation problems in atomic and molecular systems iii. rederivation of the coupled-pair many-electron theory using the traditional quantum chemical methodst. *International Journal of Quantum Chemistry*, 5(4):359–379, 1971.
- [19] J. Cizek and J. Paldus. Coupled cluster approach. *Physica Scripta*, 21(3-4):251, 1980.
- [20] Jiri Cizek. On the correlation problem in atomic and molecular systems. calculation of wavefunction components in urselltype expansion using quantumfield theoretical methods. *The Journal of Chemical Physics*, 45(11):4256–4266, 1966.
- [21] D. B. Cline, G. M. Fuller, W. P. Hong, B. Meyer, and J. Wilson. Prospects for detection of a cosmologically significant neutrino mass from a galactic supernova neutrino burst using a neutral-current-based detector. *Phys. Rev. D*, 50:720–729, Jul 1994.
- [22] F. Coester. Bound states of a many-particle system. *Nuclear Physics*, 7(Supplement C):421 – 424, 1958.
- [23] F. Coester and H. Kmmel. Short-range correlations in nuclear wave functions. *Nuclear Physics*, 17(Supplement C):477 – 485, 1960.
- [24] E. U. Condon. The theory of complex spectra. *Phys. Rev.*, 36:1121–1133, Oct 1930.
- [25] Jane Doe and John Smith. Lorem ipsum dolor sit amet, consectetur adipiscing elit. *Lor. Ips.*, 45:123, 2000.
- [26] S. R. Elliott, A. A. Hahn, and M. K. Moe. Direct evidence for two-neutrino double-beta decay in ^{82}Se . *Phys. Rev. Lett.*, 59:2020–2023, Nov 1987.
- [27] E. Epelbaum, H.-W. Hammer, and Ulf-G. Meißner. Modern theory of nuclear forces. *Rev. Mod. Phys.*, 81:1773–1825, Dec 2009.

- [28] G.T. Ewan. The sudbury neutrino observatory. *Nuclear Instruments and Methods in Physics Research Section A: Accelerators, Spectrometers, Detectors and Associated Equipment*, 314(2):373 – 379, 1992.
- [29] J. R. Gour, P. Piecuch, M. Hjorth-Jensen, M. Włoch, and D. J. Dean. Coupled-cluster calculations for valence systems around ^{16}O . *Phys. Rev. C*, 74:024310, Aug 2006.
- [30] K. Gulyuz, J. Ariche, G. Bollen, S. Bustabad, M. Eibach, C. Izzo, S. J. Novario, M. Redshaw, R. Ringle, R. Sandler, S. Schwarz, and A. A. Valverde. Determination of the direct double- β -decay q value of ^{96}Zr and atomic masses of $^{90-92,94,96}\text{Zr}$ and $^{92,94-98,100}\text{Mo}$. *Phys. Rev. C*, 91:055501, May 2015.
- [31] G. Hagen, A. Ekström, C. Forssén, G. R. Jansen, W. Nazarewicz, T. Papenbrock, K. A. Wendt, S. Bacca, N. Barnea, B. Carlsson, C. Drischler, K. Hebeler, M. Hjorth-Jensen, M. Miorelli, G. Orlandini, A. Schwenk, and J. Simonis. Neutron and weak-charge distributions of the ^{48}Ca nucleus. *Nature Physics*, 12:186 EP –, Nov 2015. Article.
- [32] G. Hagen, T. Papenbrock, M. Hjorth-Jensen, and D. J. Dean. Coupled-cluster computations of atomic nuclei. *Rep. Prog. in Phys.*, 77(9):096302, Sep 2014.
- [33] J. C. Hardy and I. S. Towner. Superaligned $0^+ \rightarrow 0^+$ nuclear β decays: A critical survey with tests of the conserved vector current hypothesis and the standard model. *Phys. Rev. C*, 71:055501, May 2005.
- [34] C.K. Hargrove, I. Batkin, M.K. Sundaresan, and J. Dubeau. A lead astronomical neutrino detector: Land. *Astroparticle Physics*, 5(2):183 – 196, 1996.
- [35] H Hergert. In-medium similarity renormalization group for closed and open-shell nuclei. *Physica Scripta*, 92(2):023002, 2017.
- [36] H. Hergert, S. Binder, A. Calci, J. Langhammer, and R. Roth. Ab initio calculations of even oxygen isotopes with chiral two-plus-three-nucleon interactions. *Phys. Rev. Lett.*, 110:242501, Jun 2013.
- [37] H. Hergert, S. K. Bogner, T. D. Morris, S. Binder, A. Calci, J. Langhammer, and R. Roth. Ab initio multireference in-medium similarity renormalization group calculations of even calcium and nickel isotopes. *Phys. Rev. C*, 90:041302, Oct 2014.
- [38] K. Hirata, T. Kajita, M. Koshiba, M. Nakahata, Y. Oyama, N. Sato, A. Suzuki, M. Takita, Y. Totsuka, T. Kifune, T. Suda, K. Takahashi, T. Tanimori, K. Miyano, M. Yamada, E. W. Beier, L. R. Feldscher, S. B. Kim, A. K. Mann, F. M. Newcomer, R. Van, W. Zhang, and B. G. Cortez. Observation of a neutrino burst from the supernova sn1987a. *Phys. Rev. Lett.*, 58:1490–1493, Apr 1987.
- [39] J. Hubbard. The description of collective motions in terms of many-body perturbation theory. *Proceedings of the Royal Society of London. Series A, Mathematical and Physical Sciences*, 240(1223):539–560, 1957.

- [40] N.M. Hugenholtz. Perturbation theory of large quantum systems. *Physica*, 23(1):481 – 532, 1957.
- [41] G. R. Jansen, J. Engel, G. Hagen, P. Navrátil, and A. Signoracci. Ab-initio coupled-cluster effective interactions for the shell model: Application to neutron-rich oxygen and carbon isotopes. *Phys. Rev. Lett.*, 113:142502, Oct 2014.
- [42] G. R. Jansen, M. D. Schuster, A. Signoracci, G. Hagen, and P. Navrátil. Open *sd*-shell nuclei from first principles. *Phys. Rev. C*, 94:011301, Jul 2016.
- [43] W. Jaus and G. Rasche. Nuclear-structure dependence of $o(\alpha)$ corrections to fermi decays and the value of the kobayashi-maskawa matrix element V_{ud} . *Phys. Rev. D*, 41:166–176, Jan 1990.
- [44] Makoto Kobayashi and Toshihide Maskawa. Cp-violation in the renormalizable theory of weak interaction. *Progress of Theoretical Physics*, 49(2):652–657, 1973.
- [45] E Kolbe, K Langanke, G Martnez-Pinedo, and P Vogel. Neutrinonucleus reactions and nuclear structure. *Journal of Physics G: Nuclear and Particle Physics*, 29(11):2569, 2003.
- [46] K. Kowalski, D. J. Dean, M. Hjorth-Jensen, T. Papenbrock, and P. Piecuch. Coupled cluster calculations of ground and excited states of nuclei. *Phys. Rev. Lett.*, 92:132501, Apr 2004.
- [47] H. Kmmel, K.H. Lhrmann, and J.G. Zabolitzky. Many-fermion theory in exps- (or coupled cluster) form. *Physics Reports*, 36(1):1 – 63, 1978.
- [48] K. Langanke, P. Vogel, and E. Kolbe. Signal for supernova ν_μ and ν_τ neutrinos in water Čerenkov detectors. *Phys. Rev. Lett.*, 76:2629–2632, Apr 1996.
- [49] David L. Lincoln, Jason D. Holt, Georg Bollen, Maxime Brodeur, Scott Bustabad, Jonathan Engel, Samuel J. Novario, Matthew Redshaw, Ryan Ringle, and Stefan Schwarz. First direct double- β decay q -value measurement of ^{82}Se in support of understanding the nature of the neutrino. *Phys. Rev. Lett.*, 110:012501, Jan 2013.
- [50] R. Machleidt and D.R. Entem. Chiral effective field theory and nuclear forces. *Physics Reports*, 503(1):1 – 75, 2011.
- [51] H. S. Miley, F. T. Avignone, R. L. Brodzinski, J. I. Collar, and J. H. Reeves. Suggestive evidence for the two-neutrino double- β decay of ^{76}Ge . *Phys. Rev. Lett.*, 65:3092–3095, Dec 1990.
- [52] P. Navrátil, J. P. Vary, and B. R. Barrett. Large-basis ab initio no-core shell model and its application to ^{12}C . *Phys. Rev. C*, 62:054311, Oct 2000.
- [53] Petr Navrtil, Sofia Quaglioni, Ionel Stetcu, and Bruce R Barrett. Recent developments in no-core shell-model calculations. *Journal of Physics G: Nuclear and Particle Physics*, 36(8):083101, 2009.

- [54] N. M. Parzuchowski, T. D. Morris, and S. K. Bogner. Ab initio excited states from the in-medium similarity renormalization group. *Phys. Rev. C*, 95:044304, Apr 2017.
- [55] Piotr Piecuch, Karol Kowalski, Ian S. O. Pimienta, and Michael J. McGuire. Recent advances in electronic structure theory: Method of moments of coupled-cluster equations and renormalized coupled-cluster approaches. *International Reviews in Physical Chemistry*, 21(4):527–655, 2002.
- [56] Steven C. Pieper, , and R. B. Wiringa. Quantum monte carlo calculations of light nuclei. *Annual Review of Nuclear and Particle Science*, 51(1):53–90, 2001.
- [57] B. S. Pudliner, V. R. Pandharipande, J. Carlson, Steven C. Pieper, and R. B. Wiringa. Quantum monte carlo calculations of nuclei with $a \leq 7$. *Phys. Rev. C*, 56:1720–1750, Oct 1997.
- [58] P. Pulay. Improved scf convergence acceleration. *J. Comput. Chem.*, 3(4):556–560, 1982.
- [59] Péter Pulay. Convergence acceleration of iterative sequences. the case of scf iteration. *Chem. Phys. Lett.*, 73(2):393 – 398, 1980.
- [60] Matthew Redshaw, Georg Bollen, Maxime Brodeur, Scott Bustabad, David L. Lincoln, Samuel J. Novario, Ryan Ringle, and Stefan Schwarz. Atomic mass and double- β -decay q value of ^{48}Ca . *Phys. Rev. C*, 86:041306, Oct 2012.
- [61] Robert Roth, Joachim Langhammer, Angelo Calci, Sven Binder, and Petr Navrátil. Similarity-transformed chiral $nn + 3n$ interactions for the ab initio description of ^{12}C and ^{16}O . *Phys. Rev. Lett.*, 107:072501, Aug 2011.
- [62] H.F. Schaefer. *Quantum chemistry: the development of ab initio methods in molecular electronic structure theory*. Oxford science publications. Clarendon Press, 1984.
- [63] I. Shavitt and R. J. Bartlett. *Many-Body Methods in Chemistry and Physics: MBPT and Coupled-Cluster Theory*. Cambridge Molecular Science. Cambridge University Press, 2009.
- [64] J. C. Slater. The theory of complex spectra. *Phys. Rev.*, 34:1293–1322, Nov 1929.
- [65] V. Somà, C. Barbieri, and T. Duguet. Ab initio gorkov-green’s function calculations of open-shell nuclei. *Phys. Rev. C*, 87:011303, Jan 2013.
- [66] V. Somà, C. Barbieri, and T. Duguet. Ab initio self-consistent gorkov-green’s function calculations of semi-magic nuclei: Numerical implementation at second order with a two-nucleon interaction. *Phys. Rev. C*, 89:024323, Feb 2014.
- [67] V. Somà, A. Cipollone, C. Barbieri, P. Navrátil, and T. Duguet. Chiral two- and three-nucleon forces along medium-mass isotope chains. *Phys. Rev. C*, 89:061301, Jun 2014.
- [68] S. R. Stroberg, A. Calci, H. Hergert, J. D. Holt, S. K. Bogner, R. Roth, and A. Schwenk. Nucleus-dependent valence-space approach to nuclear structure. *Phys. Rev. Lett.*, 118:032502, Jan 2017.

- [69] S. R. Stroberg, H. Hergert, J. D. Holt, S. K. Bogner, and A. Schwenk. Ground and excited states of doubly open-shell nuclei from ab initio valence-space hamiltonians. *Phys. Rev. C*, 93:051301, May 2016.
- [70] Jouni Suhonen and Osvaldo Civitarese. Weak-interaction and nuclear-structure aspects of nuclear double beta decay. *Physics Reports*, 300(3):123 – 214, 1998.
- [71] I S Towner and J C Hardy. The evaluation of v_{ud} , experiment and theory. *Journal of Physics G: Nuclear and Particle Physics*, 29(1):197, 2003.
- [72] I. S. Towner and J. C. Hardy. An Improved calculation of the isospin-symmetry-breaking corrections to superallowed Fermi beta decay. *Phys. Rev.*, C77:025501, 2008.
- [73] I.S. Towner. The nuclear-structure dependence of radiative corrections in superallowed fermi beta-decay. *Nuclear Physics A*, 540(3):478 – 500, 1992.
- [74] I.S. Towner. Quenching of spin operators in the calculation of radiative corrections for nuclear beta decay. *Physics Letters B*, 333(1):13 – 16, 1994.
- [75] K. Tsukiyama, S. K. Bogner, and A. Schwenk. In-medium similarity renormalization group for nuclei. *Phys. Rev. Lett.*, 106:222502, Jun 2011.
- [76] K. Tsukiyama, S. K. Bogner, and A. Schwenk. In-medium similarity renormalization group for open-shell nuclei. *Phys. Rev. C*, 85:061304, Jun 2012.
- [77] C. W. Ufford. Configuration interaction in complex spectra. *Phys. Rev.*, 44:732–739, Nov 1933.
- [78] M. Włoch, D. J. Dean, J. R. Gour, M. Hjorth-Jensen, K. Kowalski, T. Papenbrock, and P. Piecuch. Ab-initio coupled-cluster study of ^{16}O . *Phys. Rev. Lett.*, 94:212501, Jun 2005.
- [79] Marta Woch, Jeffrey R Gour, Piotr Piecuch, David J Dean, Morten Hjorth-Jensen, and Thomas Papenbrock. Coupled-cluster calculations for ground and excited states of closed- and open-shell nuclei using methods of quantum chemistry. *Journal of Physics G: Nuclear and Particle Physics*, 31(8):S1291, 2005.